

RESEARCH REPORT

**Hysteretic shear response of fasteners connecting
sheathing to cold-formed steel studs**

K.D. Peterman, B.W. Schafer

CFS-NEES – RR04

January 2013

This report was prepared as part of the U.S. National Science Foundation sponsored CFS-NEES project: NSF-CMMI-1041578: NEESR-CR: Enabling Performance-Based Seismic Design of Multi-Story Cold-Formed Steel Structures. The project also received supplementary support and funding from the American Iron and Steel Institute. Project updates are available at www.ce.jhu.edu/cfsnees. Any opinions, findings, and conclusions or recommendations expressed in this publication are those of the author(s) and do not necessarily reflect the views of the National Science Foundation, nor the American Iron and Steel Institute.

ABSTRACT

The series of experiments reported here aims to characterize the hysteretic behavior of the connection between cold-formed steel (CFS) studs and sheathing when subject to in-plane lateral demands. This connection provides the key energy dissipating behavior in wood sheathed CFS shear walls, and provides bracing to the studs under gravity and out-of-plane loads. A testing rig is developed consisting of two CFS lipped channels facing toe-to-toe connected on the flanges by sheathing (oriented strand board, or gypsum board) and cycled such that the 8 connecting fasteners experience shear. Sheathing configuration, fastener spacing, steel thickness, and fastener type are varied to determine connection performance. The dominant role of sheathing type and stud thickness is highlighted in the results. The hysteretic behavior of the experimental results is summarized for further use in the analysis of shear walls and under gravity and lateral load. The work serves as a supplement to North American efforts to advance seismic performance-based design of CFS structures and is part of a larger effort to better understand CFS lateral force resisting systems.

Keywords: cold-formed steel, thin-walled structures, cyclic response, fastener response

TABLE OF CONTENTS

ABSTRACT	3
1. INTRODUCTION	5
2. TEST METHODOLOGY	5
<i>2.1 Test Setup</i>	5
<i>2.2 Test Parameters</i>	8
3. MATERIAL PROPERTIES	9
4. RESULTS AND DISCUSSION	10
<i>4.1 Conversion to Single Fastener Values</i>	10
<i>4.2 Monotonic Test Results</i>	11
<i>4.3 Cyclic Test Results</i>	12
5. HYSTERETIC CHARACTERIZATION	17
6. RECOMMENDATIONS	21
7. CONCLUSIONS	23
ACKNOWLEDGEMENTS	23
REFERENCES	24
APPENDICES	25
<i>Appendix A: Specimen Information Sheets</i>	25
<i>Appendix B: Tensile Test Results</i>	38

1. INTRODUCTION

Cold-formed steel is gaining momentum in the low-to-mid-rise construction industry as a lightweight yet strong material that is economically efficient. While there is a large body of existing research in cold-formed steel, this specific research is largely motivated by the National Science Foundation funded Network for Earthquake Engineering Simulation (NEES) project: CFS-NEES (www.ce.jhu.edu/cfsnees). CFS-NEES aims to improve the performance-based seismic design of cold-formed steel structures and culminates in the construction and testing of a two-story full-scale cold-formed steel building (termed the CFS-NEES building), to be tested at the University of Buffalo in 2013. The CFS-NEES project aims to better characterize and understand the behavior of cold-formed steel systems through computational models and experimental tests.

The experimental work presented here focuses on the lateral performance of the stud-fastener-sheathing connection. The selected test parameters are drawn from common North American construction methods, and also from the shear wall construction in the fully detailed archetype CFS-NEES building (Madsen et al. 2011). Previously, tests of the full CFS-NEES shear walls were conducted at the University of North Texas (Liu et al., 2012). The goal of the stud-fastener-sheathing connection tests reported here is to provide the hysteretic response and subsequent characterization of the fastener response for computational modeling of shear walls built up from the fundamental fastener response similar to efforts in previous wood research (Folz and Filiatrault (2001, 2002, 2004)). The long-term goal of this work is to enable a mechanics-based method for building up the lateral response of any sheathed cold-formed steel system: shear wall, diaphragm, etc. for situations where testing is not practical or available.

2. TEST METHODOLOGY

2.1 Test Setup

A specimen and the testing rig are illustrated in **Figure 1**. The testing rig design is influenced by the early work of Winter (Green et al (1947)) to characterize lateral stiffness in sheathed stud walls as well as the more recent cyclic work of Fiorino et al. (2007) and the monotonic tests of Vieira and Schafer (2012). The specimen is connected

to the rig via the stud web, which is bolted to a steel base plate on the rig. Steel plates (**Figure 1(c)**) restrict the web from movement, ensuring that the connection forces are limited to the channel flange. The top of the rig (**Figure 1(a)**) is fixed, both translationally and torsionally. The bottom, where the load is applied, is torsionally free, albeit restrained by the sheathing until post-peak.

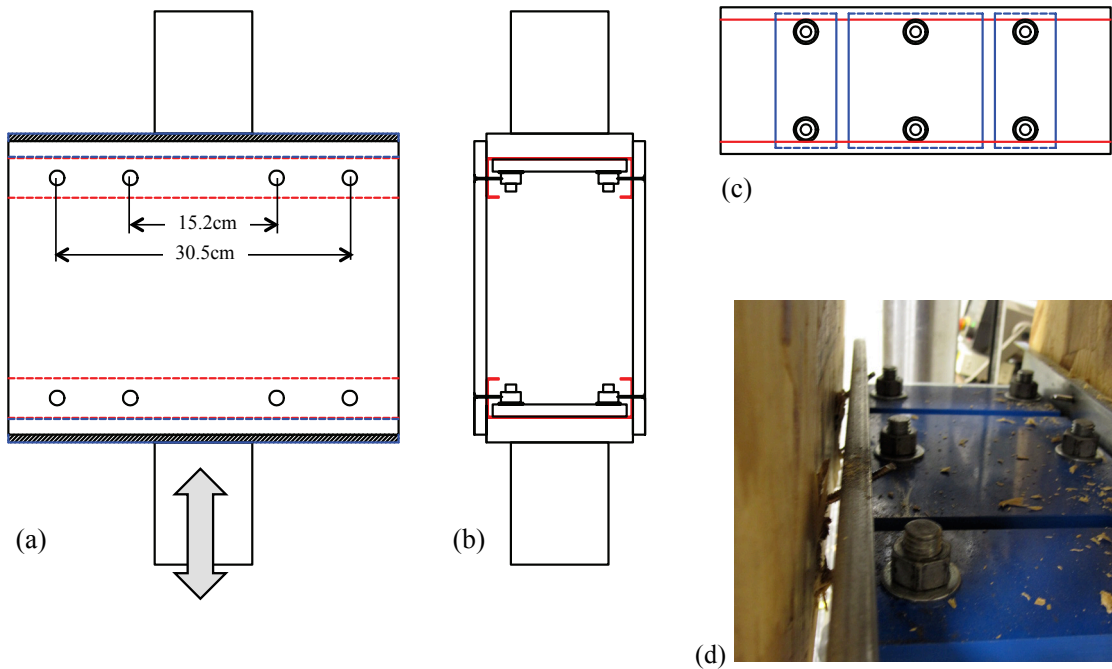


Figure 1 (a) Front view of loaded specimen, dashed lines indicate hidden stud, arrow indicates location and direction of loading (b) Side view of specimen in rig (c) Inside view of stud clamping system (d) photograph of clamping system

Loading in the tests was either monotonic, or cyclic (following the CUREE protocol). The monotonic tests are required for determining the target displacements in the CUREE cyclic protocol, as illustrated in Figure 2 for a sample cyclic CUREE protocol based on reference displacement Δ , which is 60% of the displacement from a monotonic test occurring at 80% of the peak load. Load rate was constant throughout the test at one full cycle every 16 seconds.

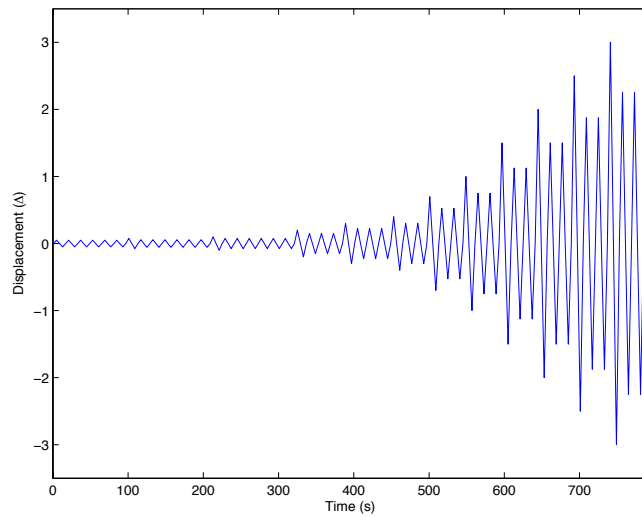


Figure 2 CUREE protocol based upon reference displacement Δ , as determined from monotonic tests.

This testing rig provides the response of eight stud-fastener-sheathing combinations in shear. The direction of shear is perpendicular to the stud flange. In shear walls the primary shear direction in the chord studs is parallel to the stud flanges. The stud deformations are localized to the flange and the OSB and Gypsum sheathing do not have preferential material response in a specific direction, therefore it is assumed that stud-fastener-sheathing response in shear parallel and perpendicular to the stud flange is the same. For studies of edge distance effects or the impact of sheathing orientation (for example, parallel or perpendicular to the grain) this assumption needs to be treated with care.

In the test setup, (without modification) the fasteners may tilt and under large deformations the tips of the fasteners bear against the web of the channel. In practice, the tilting would be parallel to the stud flange and never engage in this bearing mode. Furthermore, even for shear perpendicular to the flange this bearing is dependent on fastener length and not considered to be a reliable secondary load path. To avoid this unrealistic bearing, 1/2 inch at the end of each fastener was ground off after being driven through the sheathing. Gaps in the stud clamping system (**Figure 1(c)**) permitted full fastener movement, at both fastener spacings and bearing of the fastener tips did not occur in the tests.

2.2 Test Parameters

Specimens were configured to represent two scenarios: common North American light steel framing construction and typical shear wall assemblies in the CFS-NEES model building. For these purposes, a 6 inch deep cold-formed steel channel section was chosen as the standard dimensions (600S162 in AISI S200-07 notation). Three nominal steel thicknesses were tested: 33, 54, and 97 mil. To capture behavior of both chord and field studs in a shear wall, two fastener spacings were also tested: 12 inches to simulate a field stud, and 6 inches to simulate a chord stud. Furthermore, sheathing type was varied between 7/16 inch thick oriented strand board (OSB, Georgia Pacific Brand, APA rated 24/16, exposure 1) and 1/2 inch thick Gypsum board (USG Sheetrock brand). Sheathing samples were kept at standard temperature and humidity (25C and 50% relative humidity) in an environmental chamber for seven days to normalize sheathing behavior. This test series employed Simpson Strong Tie QuikDrive fasteners: #8 for OSB-to-steel and #6 for gypsum-to-steel. AISI-S100 requires a minimum edge distance of 1.5 times the diameter of the faster (in both cases $>0.2''$); to avoid edge tear out, fasteners were located 1.5 inch from the top of the sheathing and at the approximate flange center. The test parameters are summarized in the test matrix of Table 1.

Table 1 Basic test matrix for characterizing fastener response in shear

		6" Spacing		12" Spacing	
<i>Loading</i>		<i>OSB</i>	<i>Gypsum</i>	<i>OSB</i>	<i>Gypsum</i>
33 mil	<i>Monotonic</i>	2*	2	2	2
	<i>CUREE</i>	2	2	2	2
54 mil	<i>Monotonic</i>	2	2	2	2
	<i>CUREE</i>	2	2	2	2
97 mil	<i>Monotonic</i>	2	2	2	2
	<i>CUREE</i>	2	2	2	2

*indicates number of specimens

Note, for the raw data and in the appendices an abbreviated nomenclature is employed. This nomenclature is summarized below and detailed in the following: the first character, either c (cyclic) or m (monotonic) corresponds to the type of loading; the second two numbers refer to steel thickness: either 33, 54, or 97 mil steel; following this, the fourth

character, either g (Gypsum board) or o (OSB) refers to sheathing type; the fifth number details whether the fasteners were spaced twelve inches apart (12) or six inches apart (6); and finally, specimen repetitions are denoted by a 1 or 2 at the end of the specimen name.

Test Name Nomenclature	
c54g12_2	= cyclic test (c), 54mil steel (54), gypsum sheathing (g), 12" fastener spacing (12), repetition 2 (2)
c97o6_1	= cyclic test (c), 97mil steel (97), OSB sheathing (o), 6" fastener spacing (6), repetition 1 (1)

3. MATERIAL PROPERTIES

Tensile coupons were cut from the flanges of the channel sections used in the tests Figure 3 and the tensile specimens were loaded until failure.

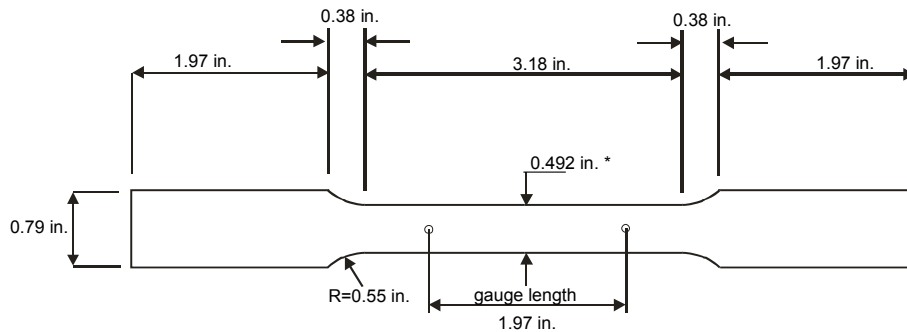


Figure 3 Tensile Coupon (Moen, 2008)

Complete stress-strain curves are provided in Appendix B, but Table 2 summarizes the basic material properties: yield stress, ultimate stress, and maximum ductility.

Table 2 Summary of material properties

Specimen	Steel Thick. ¹	Yield Stress	Ult. Stress	Ult. Strain
-	<i>t</i>	F_y	F_u	ϵ_u
-	in.	ksi	ksi	in./in.
1a (33mil)	0.0375	40.1	50.8	0.186
1b (33mil) ²	0.0375	--	--	--
2a (54mil)	0.0573	51.5	65.1	0.188
2b (54mil)	0.0573	52.1	64.9	0.191
3a (97mil)	0.0995	58	75.8	0.167
3b (97mil)	0.1	58.8	75.5	0.167

¹coated thickness ²extensometer hardware errors resulted in unusable data

Additional material properties testing on the fasteners, or sheathing, was not conducted.

4. RESULTS AND DISCUSSION

4.1 Conversion to Single Fastener Values

Conversion of the full test results, on eight fasteners, to single fastener values are derived in Vieira and Schafer (2009). The key free body diagrams are provided in Figure 4 and Figure 5:

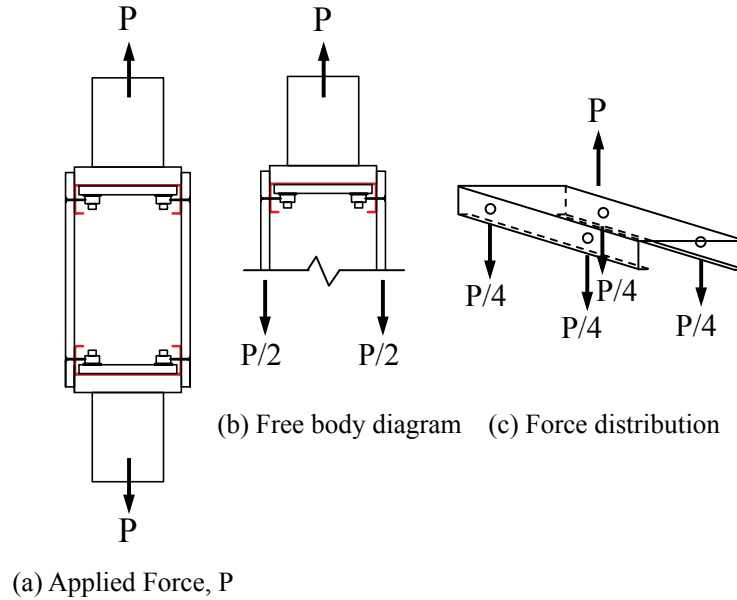


Figure 4 Free-body diagrams for determination of individual fastener forces, P_i

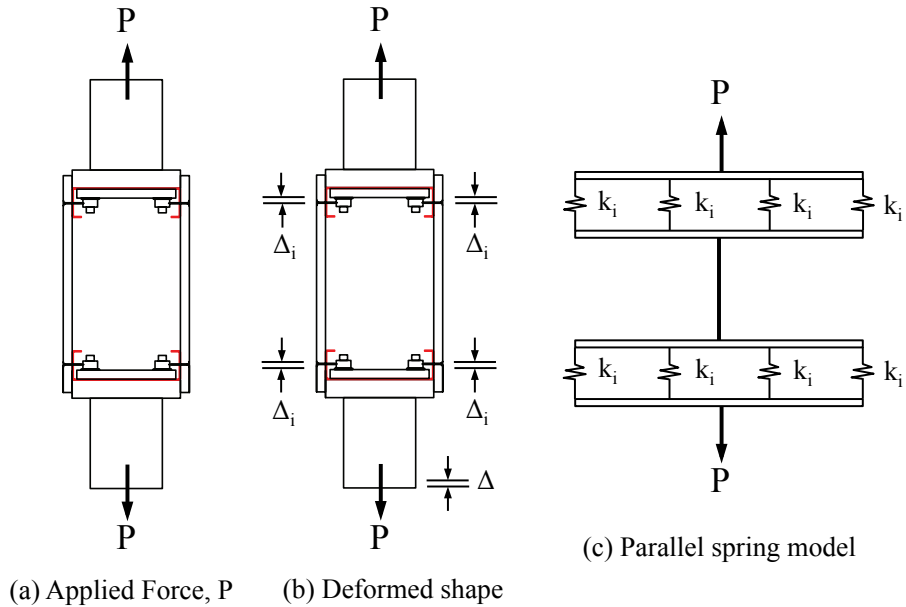


Figure 5 Free-body diagram for determination of individual fastener stiffness, k_i

The individual fastener force, P_i , assuming a total applied force of P , is $P_i = P/4$. Assuming all deformations occur at the fastener locations implies that the deformation at the fastener, Δ_i , is determined from the total deformation Δ , as $\Delta_i = \Delta/2$. Fastener stiffness then becomes: $k_i = K/2$.

4.2 Monotonic Test Results

Typical force-deformation results for two nominally identical specimens under monotonic loading are provided in Figure 6. Scatter in the response is non-trivial. Force-deformation results for all monotonic tests are provided in Appendix A. The initial system stiffness (K) is determined by the secant stiffness to $0.40P_{max}$ per Krawinkler, et al (2000), as illustrated in Figure 4.1.3 for two nominally identical specimens. The reference displacement for the CUREE protocol, Δ_m , which is 60% of the displacement from a monotonic test occurring at $0.80P_{max}$ is also determined for each specimen. Average Δ_m results for nominally identical specimens are utilized in the subsequent cyclic (CUREE protocol) tests.

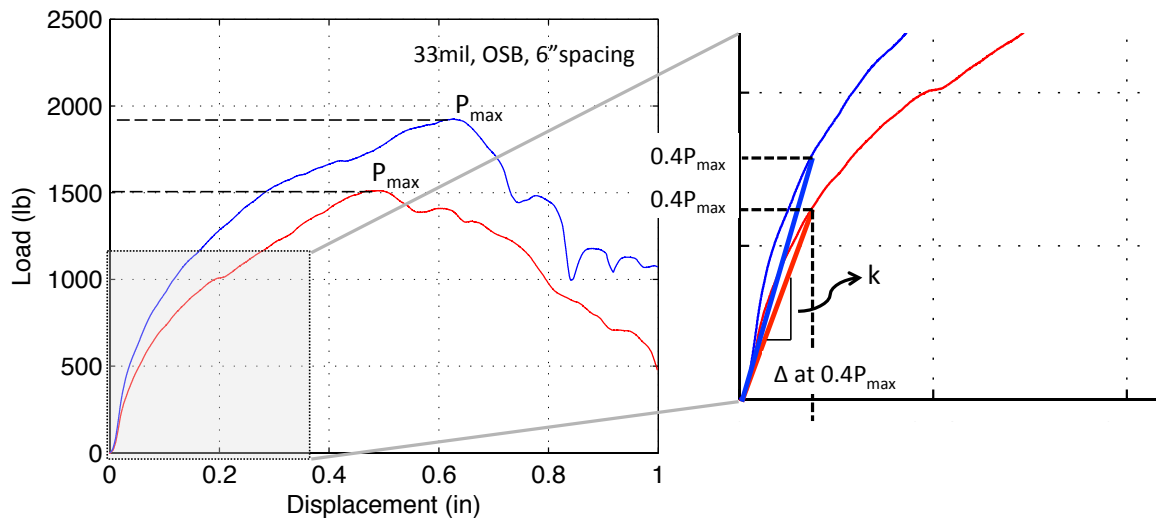


Figure 6 Graphical summary of procedure to determine initial system stiffness for a monotonic test, results from two nominally identical specimens are illustrated.

Key test results for all conducted monotonic tests are provided in Table 3. Although significant scatter exists in the test results some basic findings are immediately clear: lateral strength and stiffness for a fastener in OSB is far greater than gypsum. The stud

thickness is strongly correlated with initial lateral stiffness of the assembly (thicker studs implying stiffer lateral response), but not necessarily peak strength. For example, the 97 mil specimens with OSB sheathing fail in screw shear, instead of pull-through and bearing, and result in lower peak strength and lower maximum displacement at failure than the same screws in 54 mil studs. Fastener spacing (at least between 6 inches and 12 inches) is not influential in determining the strength. As will be shown, these observations generally hold in the cyclic test results to follow.

Table 3 Summary of monotonic test results

sheathing	steel thickness	fastener spacing	peak load	stiffness	disp. at peak	ref. disp.	single fastener values			Test Name	
							P_{max-i}	Δ_{max-i}	k_i		
	mil	in.	kips	kips/in.	in.	in.	kips	in.	kips/in.		
OSB	33	6	1.51	8.48	0.50	0.74	0.38	0.25	4.24	m33o6-1	
		6	1.93	10.90	0.63	0.73	0.48	0.31	5.45	m33o6-2	
		12	1.78	10.00	0.54	0.75	0.45	0.27	5.00	m33o12-1	
		12	1.86	9.39	0.73	0.90	0.47	0.37	4.70	m33o12-2	
	54	6	1.77	19.64	0.48	0.60	0.44	0.24	9.82	m54o6-1	
		6	2.06	15.20	0.59	0.71	0.51	0.29	7.60	m54o6-2	
		12	2.25	18.94	0.59	0.70	0.56	0.29	9.47	m54o12-1	
		12	1.72	15.87	0.49	0.61	0.43	0.24	7.94	m54o12-2	
	97	6	1.41	23.90	0.18	0.30	0.35	0.09	11.95	m97o6-1	
		6	1.43	22.71	0.14	0.25	0.36	0.07	11.36	m97o6-2	
		12	1.64	19.40	0.22	0.29	0.41	0.11	9.70	m97o12-1	
		12	1.34	20.67	0.26	0.31	0.33	0.13	10.34	m97o12-2	
		12	1.69	21.81	0.18	0.24	0.42	0.09	10.91	m97o12-3	
	Gypsum	33	6	0.49	6.56	0.60	0.78	0.12	0.30	3.28	m33g6-1
			6	0.44	6.50	0.48	0.73	0.11	0.24	3.25	m33g6-2
12			0.43	6.22	0.63	0.75	0.11	0.32	3.11	m33g12-1	
12			0.48	8.45	0.64	0.88	0.12	0.32	4.23	m33g12-2	
54		6	0.55	6.92	0.53	0.73	0.14	0.26	3.46	m54g6-1	
		6	0.49	4.69	0.69	0.74	0.12	0.34	2.35	m54g6-2	
		12	0.47	8.37	0.54	0.62	0.12	0.27	4.19	m54g12-1	
		12	0.48	8.07	0.30	0.62	0.12	0.15	4.04	m54g12-2	
97		6	0.40	6.55	0.10	0.20	0.10	0.05	3.28	m97g6-1	
		6	0.50	9.86	0.56	0.73	0.12	0.28	4.93	m97g6-2	
		12	0.46	11.92	0.18	0.40	0.11	0.09	5.96	m97g12-1	
		12	0.40	5.26	0.47	0.59	0.10	0.24	2.63	m97g12-2	

4.3 Cyclic Test Results

Typical force-deformation results as the CUREE load protocol is followed are provided in Figure 7(a) for a specimen with 54 mil steel studs, OSB sheathing, and 6 inch fastener spacing. The response is severely pinched with essentially no force in the second and fourth quadrants of the force-deformation space. This is indicative of the fact that bearing of the screw into the sheathing (pivoting about the connection to the stud) is the primary

mode of resistance. Though more difficult to discern directly from the force-deformation, but consistent with the bearing resistance mechanism, re-loading does not occur until a significant portion of the previous maximum deformation has been obtained. The cyclic force-deformation performance of all specimens is provided in Appendix A.

Initial backbone curves (envelope curves in the force-deformation response) were constructed for each specimen hysteresis, utilizing the response at 40% peak load, 80% peak load, peak load, and the last stable loop. For example, see Figure 7(a) for the backbone of the specimen with 54 mil steel studs, OSB sheathing, and 6 inch fastener spacing, or see Appendix A for all other specimens. While unable to capture complete specimen response, backbone curves are useful for general comparisons between specimen types and are the first step in constructing the hysteretic response.

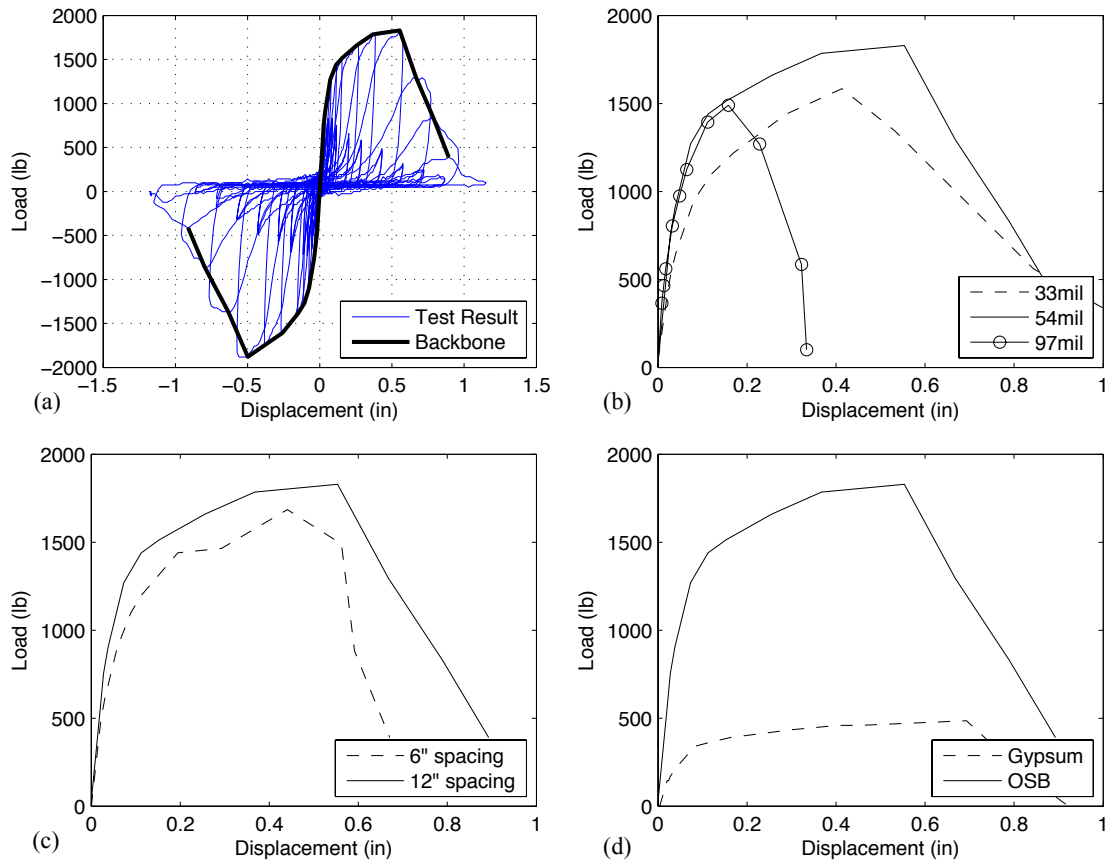


Figure 7 Backbone curve comparison around base-case specimen (54 mil steel, OSB, 6 inch spacing) (a) base case hysteresis and backbone curve (b) effect of variation in steel thickness (c) effect of fastener spacing and (d) effect on sheathing type. (Values are per-system)

Figure 7(b)-(d) provides a comparison of the backbone curve response between the baseline case of 54 mil steel studs, with OSB sheathing, and 6 inch fastener spacing. This case was selected based upon common shear wall configurations in the CFS-NEES model building. Figure 7(b) demonstrates the effect of steel thickness on the backbone response: as in the monotonic tests thicker is not always better as a transition from pull-through and bearing to screw shear occurs. Figure 7(c) compares fastener spacing, and indicates only minor differences with the two different fastener spacing. Figure 7(d) demonstrates the obvious conclusion that sheathing type not stud thickness or fastener spacing is the dominant parameter.

A more quantitative comparison of the cyclic response, for key parameters only, is provided in Table 4. These overall results are similar to the monotonic results. Stud thickness directly influences initial stiffness, but peak strength and maximum displacements can be cutoff by undesirable failure modes (screw shear in the 97 mil, OSB-sheathed specimens). Scatter is significant. The response parameters of Table 4 are averaged across the different fastener spacing and the statistics provided in Table 5. Using the CoV (standard deviation divided by the mean) as a measure of scatter, one can see that scatter in the response of gypsum-sheathed specimens is greater (as expected) than OSB sheathed specimens. Initial stiffness in OSB has a CoV of approximately 10% while gypsum has a CoV of approximately 30%. Peak capacity (strength) has the least scatter and is about 10% for all specimens, but peak displacement particularly in gypsum-sheathed specimens is so large as to make the quantity useless as an engineering parameter (CoV as high as 60%).

Table 4 Summary of key cyclic test results

sheathing	steel thickness	fastener spacing	initital	max +	max -	max +	max -	average	average	Test name
			stiffness	load	load	disp.	disp.	max load	max disp	
			K_o	P_+	P_-	Δ_+	Δ_-	P_{ave}	Δ_{ave}	-
			kips/in.	kips	kips	in.	in.	kips	in.	-
OSB	33	6	16.45	1.390	-1.564	0.429	-0.420	1.477	0.419	c33o6_1
		6	19.82	1.587	-1.537	0.426	-0.419	1.562	0.406	c33o6_2
		12	13.02	1.170	-1.245	0.337	-0.480	1.197	0.390	c33o12_1
		12	18.56	1.459	-1.589	0.480	-0.482	1.524	0.471	c33o12_2
	54	6	23.28	1.489	-1.779	0.384	-0.484	1.634	0.376	c54o6_1
		6	27.45	1.827	-1.882	0.553	-0.558	1.854	0.526	c54o6_2
		12	23.95	1.819	-1.794	0.435	-0.441	1.807	0.438	c54o12_1
		12	22.95	1.687	-1.757	0.440	-0.435	1.709	0.432	c54o12_2
	97	6	41.95	1.467	-1.512	0.158	-0.240	1.489	0.193	c97o6_1
		6	39.52	1.709	-1.684	0.114	-0.160	1.697	0.111	c97o6_2
		12	40.68	1.832	-1.882	0.113	-0.160	1.857	0.131	c97o12_1
		12	41.45	1.902	-1.782	0.161	-0.159	1.832	0.130	c97o12_2
Gypsum	33	6	6.85	0.370	-0.385	0.309	-0.304	0.377	0.303	c33g6_1
		6	5.55	0.390	-0.320	0.444	-0.308	0.355	0.294	c33g6_2
		12	9.84	0.435	-0.370	0.445	-0.681	0.402	0.496	c33g12_1
		12	7.83	0.365	-0.440	0.321	-0.454	0.402	0.298	c33g12_2
	54	6	12.04	0.515	-0.510	0.963	-1.274	0.512	0.921	c54g6_1
		6	6.12	0.483	-0.567	0.736	-1.286	0.525	0.914	c54g6_2
		12	15.28	0.512	-0.467	0.427	-1.028	0.477	0.458	c54g12_1
		12	14.53	0.380	-0.500	0.436	-0.891	0.440	0.357	c54g12_2
	97	6	18.80	0.560	-0.465	0.373	-0.772	0.502	0.410	c97g6_1
		6	10.07	0.485	-0.490	0.676	-0.836	0.487	0.644	c97g6_2
		12	12.26	0.430	-0.475	0.117	-0.203	0.452	0.138	c97g12_1
		12	15.28	0.532	-0.442	0.348	-0.869	0.477	0.337	c97g12_2

* divide forces by 4 and displacements by 2 to convert to single fastener values (P_i, Δ_i)

Table 5 Key cyclic test results averaged across fastener spacing

sheathing	steel thickness		initital	max +	max -	max +	max -	average	average
			stiffness	load	load	disp.	disp.	max load	max disp
			K_o	P_+	P_-	Δ_+	Δ_-	P_{ave}	Δ_{ave}
			kips/in.	kips	kips	in.	in.	kips	in.
OSB	33	mean	16.96	1.40	-1.48	0.42	-0.45	1.44	0.42
		CoV	0.18	0.12	0.11	0.14	0.08	0.12	0.08
	54	mean	24.41	1.71	-1.80	0.45	-0.48	1.75	0.44
		CoV	0.08	0.09	0.03	0.16	0.12	0.06	0.14
	97	mean	40.90	1.73	-1.71	0.14	-0.18	1.72	0.14
		CoV	0.03	0.11	0.09	0.20	0.22	0.10	0.25
Gypsum	33	mean	7.52	0.39	-0.38	0.38	-0.44	0.38	0.35
		CoV	0.24	0.08	0.13	0.20	0.41	0.06	0.28
	54	mean	11.99	0.47	-0.51	0.64	-1.12	0.49	0.66
		CoV	0.35	0.13	0.08	0.40	0.17	0.08	0.45
	97	mean	14.10	0.50	-0.47	0.38	-0.67	0.48	0.38
		CoV	0.27	0.11	0.04	0.61	0.47	0.04	0.55

One subtle aspect of the test results (see Table 4 and Table 5) is that maximum positive and negative displacement is approximately equal in the OSB sheathed specimens, but unequal in the gypsum sheathed specimens. This may be observed directly in the hysteretic response as well, as shown in Figure 8. In gypsum, under positive

displacements the fastener bears and travels across the sheathing until it tears out at an edge. For negative displacements the fasteners travel towards the center of the board--the board provides the same resistance to each cycle. Figure 8(b) highlights this behavior: the lower left quadrant plateaus, while the upper right quadrant degrades due to edge tear out. This response was observed for all gypsum specimens.

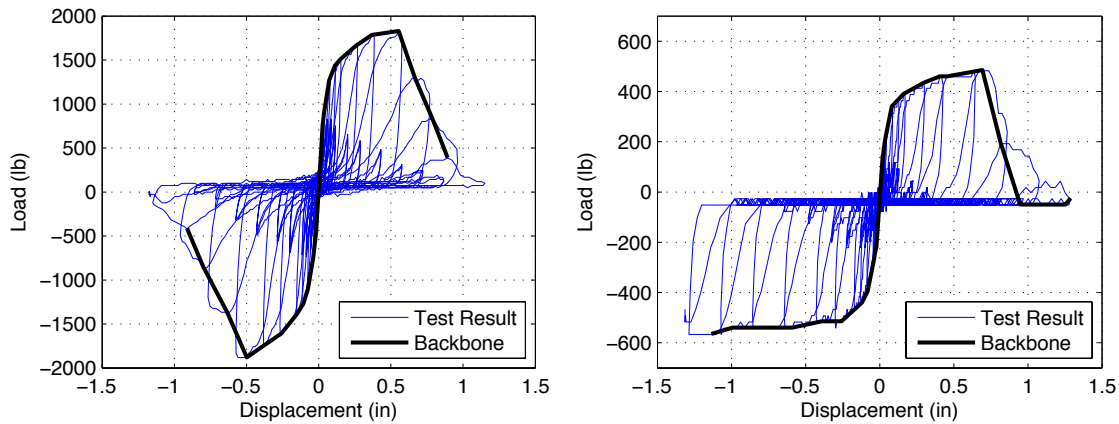


Figure 8 Hysteretic responses and backbone curves for (a) base-case specimen (54 mil steel, OSB, 6 inch spacing) and (b) gypsum variant of base-case specimen (54 mil steel, gypsum, 6 inch spacing). Note differing load scales. (Values are per-system)

5. HYSTERETIC CHARACTERIZATION

To provide a hysteretic characterization of the stud-fastener-sheathing performance appropriate for implementation in finite element models characterization via the Pinching4 model, as implemented in OpenSees, is pursued (Lowes, et al. 2004). Pinching4 parameters include four positive and negative points along the backbone, in addition to parameters that define the “pinched” or unloading/re-loading behavior of the model, as depicted in Figure 9.

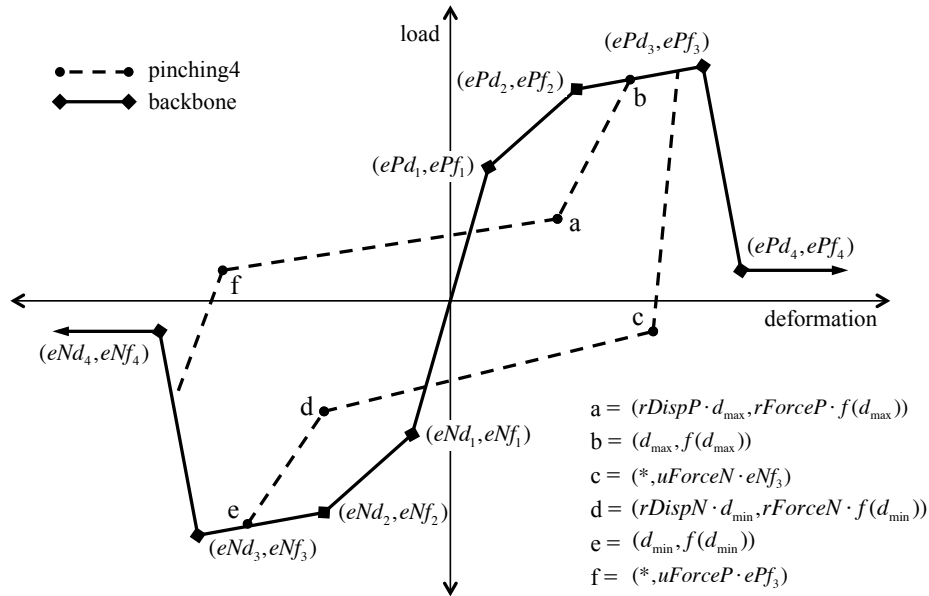


Figure 9 Pinching4 hysteresis parameters

The pinching parameters ($rDispP$, $rForceP$, $uForceN$, etc.) are based upon ratios of deformation (Disp) or force (Force) to maximum (P) or minimum (N) historic demands at various points in the unloading (u)-reloading (r) curve. The resulting hysteresis may be symmetric, or unsymmetric depending on the selected parameters. A typical comparison of the fitted Pinching4 model to the test data is provided in Figure 10 and graphical results for every test are provided in Appendix A.

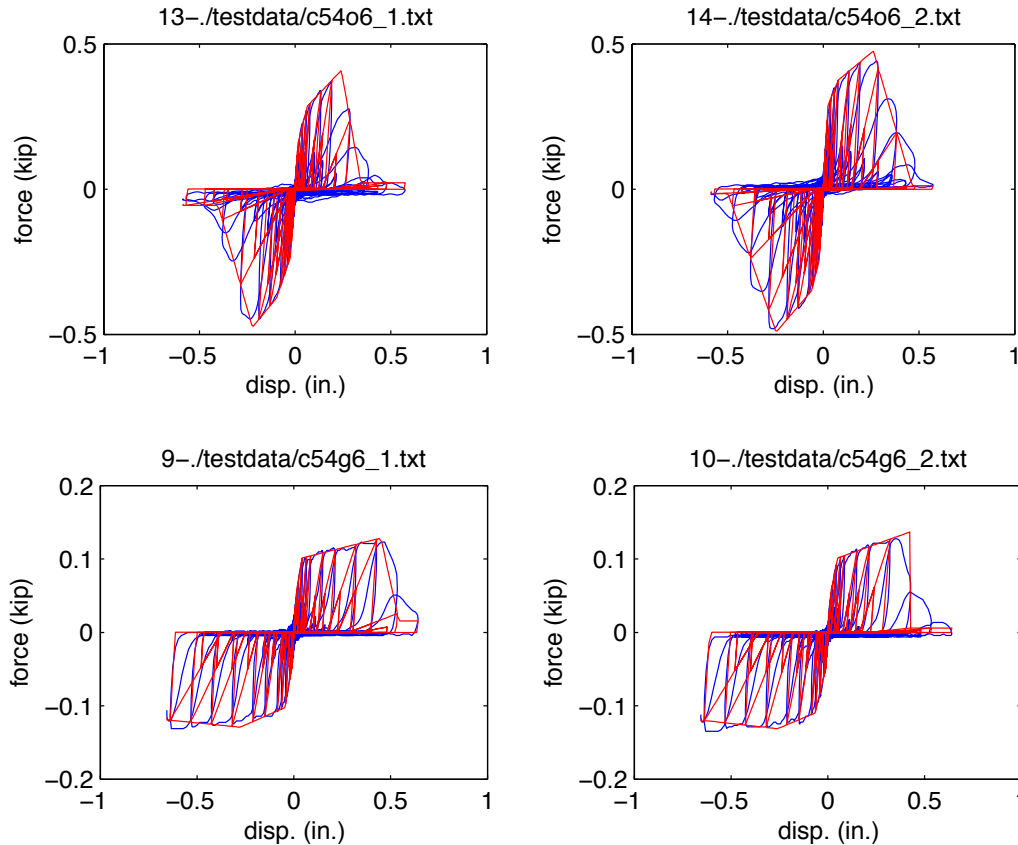


Figure 10 Comparison of test force-deformation response (blue) with fitted Pinching4 model (red) for the 54mil OSB-sheathed specimens at 6 inch fastener spacing (top) and 54mil gypsum-sheathed specimens at 6” fastener spacing (bottom).

Determination of the Pinching4 parameters, for the test data, is completed by an error minimization process. First, the backbone of the Pinching4 model is fit such that the sum squared error in the force prediction is minimized. Second, the un- and re-loading parameters of the Pinching4 model are then fit such that the sum squared error in the per cycle energy is minimized. This method ensures that two important modeling parameters, force and hysteretic energy, are accurately captured. Matlab was employed for minimizing the sum-squared error – specifically, the simplex method employed in the `fminsearch` routine (Matlab, 2002). Initial conditions used in the backbone fit were points on the experimental backbone at: 40%peak, 80%peak, peak, and the extreme recorded displacement, for both positive and negative cycles. Initial conditions in the un- and re-loading fit were taken as $r_{dispP}=r_{dispN}=0.5$ and $r_{ForceP}=r_{ForceN}=0.01$; furthermore, $u_{ForceP}=u_{ForceN}=0.001$ were fixed to insure no forces were measured in the second and

fourth quadrants of the force-displacement space. This assumption is consistent with observed test behavior.

Table 6 reports the unloading and reloading parameters for the fitted Pinching4 model and Table 7 reports the backbone curve, both negative (Table 7(b)) and positive (Table 7 (a)), for the fitted Pinching4 model.

Table 6 Unloading and reloading parameters for Pinching4 model (per fastener values)

sheathing	steel thickness	fastener spacing	rDispP	rForceP	uForceP	rDispN	rForceN	uForceN	Test Name
-	mil	in.	-	-	-	-	-	-	-
OSB	33	6	0.481	0.011	0.001	0.333	0.011	0.001	c33o6_1
		6	0.322	0.010	0.001	0.482	0.011	0.001	c33o6_2
		12	0.506	0.016	0.001	-0.123	0.012	0.001	c33o12_1
		12	0.482	0.011	0.001	0.325	0.011	0.001	c33o12_2
	54	6	0.498	0.012	0.001	0.104	0.011	0.001	c54o6_1
		6	0.503	0.014	0.001	0.115	0.012	0.001	c54o6_2
		12	0.488	0.011	0.001	0.403	0.011	0.001	c54o12_1
		12	0.496	0.011	0.001	0.281	0.011	0.001	c54o12_2
	97	6	0.500	0.013	0.001	0.164	0.011	0.001	c97o6_1
		6	0.529	0.014	0.001	-0.032	0.012	0.001	c97o6_2
		12	0.510	0.010	0.001	-0.198	0.014	0.001	c97o12_1
		12	0.590	0.009	0.001	-0.013	0.011	0.001	c97o12_2
gypsum	33	6	0.492	0.010	0.001	0.400	0.010	0.001	c33g6_1
		6	0.490	0.012	0.001	0.322	0.011	0.001	c33g6_2
		12	0.420	0.011	0.001	0.490	0.010	0.001	c33g12_1
		12	0.506	0.014	0.001	0.096	0.012	0.001	c33g12_2
	54	6	0.536	0.009	0.001	0.590	0.009	0.001	c54g6_1
		6	0.516	0.009	0.001	0.568	0.010	0.001	c54g6_2
		12	0.526	0.010	0.001	0.534	0.010	0.001	c54g12_1
		12	0.556	0.010	0.001	0.565	0.010	0.001	c54g12_2
	97	6	0.556	0.008	0.001	0.616	0.009	0.001	c97g6_1
		6	0.723	0.011	0.001	0.622	0.009	0.001	c97g6_2
		12	0.526	0.010	0.001	0.533	0.010	0.001	c97g12_1
		12	0.552	0.010	0.001	0.574	0.010	0.001	c97g12_2

Table 7 Pinching4 characterization of specimens (per fastener values)

(a) Positive backbone points

sheathing	steel thickness	fastener spacing	eNd4	eNd3	eNd2	eNd1	eNf4	eNf3	eNf2	eNf1	Test Name
-	mil	in.	in.	in.	in.	in.	kip	kip	kip	kip	-
OSB	33	6	0.018	0.069	0.241	0.540	0.158	0.298	0.371	0.021	c33o6_1
		6	0.021	0.092	0.227	0.495	0.175	0.327	0.400	0.033	c33o6_2
		12	0.021	0.050	0.207	0.446	0.142	0.211	0.327	-0.013	c33o12_1
		12	0.017	0.081	0.262	0.558	0.143	0.306	0.383	0.035	c33o12_2
	54	6	0.016	0.064	0.241	0.344	0.160	0.286	0.409	0.022	c54o6_1
		6	0.024	0.077	0.262	0.463	0.287	0.375	0.476	0.011	c54o6_2
		12	0.019	0.077	0.230	0.427	0.207	0.381	0.475	0.054	c54o12_1
		12	0.019	0.071	0.266	0.359	0.202	0.338	0.436	0.049	c54o12_2
	97	6	0.011	0.041	0.084	0.229	0.164	0.313	0.359	0.015	c97o6_1
		6	0.012	0.035	0.052	0.132	0.203	0.376	0.443	0.011	c97o6_2
		12	0.011	0.036	0.067	0.121	0.218	0.405	0.475	0.049	c97o12_1
		12	0.010	0.030	0.074	0.104	0.197	0.370	0.529	0.045	c97o12_2
gypsum	33	6	0.016	0.045	0.169	0.665	0.044	0.071	0.086	0.014	c33g6_1
		6	0.013	0.061	0.222	0.727	0.038	0.072	0.096	0.000	c33g6_2
		12	0.011	0.034	0.190	0.687	0.047	0.086	0.106	0.000	c33g12_1
		12	0.003	0.037	0.185	0.495	0.046	0.079	0.097	-0.007	c33g12_2
	54	6	0.013	0.042	0.449	0.543	0.052	0.101	0.128	0.016	c54g6_1
		6	0.017	0.051	0.423	0.423	0.058	0.101	0.137	0.006	c54g6_2
		12	0.010	0.042	0.184	0.469	0.054	0.105	0.122	0.014	c54g12_1
		12	0.008	0.037	0.157	0.444	0.045	0.087	0.104	0.061	c54g12_2
	97	6	0.007	0.043	0.211	0.321	0.046	0.112	0.129	0.053	c97g6_1
		6	0.000	0.045	0.320	0.526	0.020	0.107	0.121	0.017	c97g6_2
		12	0.005	0.019	0.037	0.436	0.041	0.078	0.102	0.020	c97g12_1
		12	0.007	0.038	0.212	0.472	0.041	0.109	0.125	0.047	c97g12_2

(b) Negative backbone points

sheathing	steel thickness	fastener spacing	eNd4	eNd3	eNd2	eNd1	eNf4	eNf3	eNf2	eNf1	Test Name
-	mil	in.	in.	in.	in.	in.	kip	kip	kip	kip	-
OSB	33	6	-0.494	-0.267	-0.077	-0.024	-0.052	-0.427	-0.313	-0.211	c33o6_1
		6	-0.476	-0.270	-0.104	-0.018	-0.016	-0.406	-0.355	-0.159	c33o6_2
		12	-0.447	-0.266	-0.085	-0.019	-0.018	-0.324	-0.248	-0.123	c33o12_1
		12	-0.491	-0.287	-0.115	-0.021	-0.050	-0.415	-0.355	-0.185	c33o12_2
	54	6	-0.402	-0.223	-0.097	-0.025	-0.056	-0.475	-0.374	-0.234	c54o6_1
		6	-0.498	-0.247	-0.061	-0.022	-0.016	-0.492	-0.350	-0.245	c54o6_2
		12	-0.445	-0.258	-0.114	-0.019	-0.065	-0.466	-0.361	-0.204	c54o12_1
		12	-0.376	-0.241	-0.059	-0.020	-0.118	-0.457	-0.310	-0.219	c54o12_2
	97	6	-0.234	-0.112	-0.049	-0.012	-0.004	-0.380	-0.361	-0.194	c97o6_1
		6	-0.135	-0.078	-0.043	-0.011	0.000	-0.419	-0.417	-0.214	c97o6_2
		12	-0.132	-0.088	-0.040	-0.010	-0.038	-0.494	-0.432	-0.197	c97o12_1
		12	-0.179	-0.101	-0.040	-0.011	-0.057	-0.475	-0.421	-0.202	c97o12_2
gypsum	33	6	-0.658	-0.170	-0.043	-0.012	-0.041	-0.104	-0.067	-0.039	c33g6_1
		6	-0.780	-0.190	-0.105	-0.018	-0.015	-0.090	-0.080	-0.045	c33g6_2
		12	-0.492	-0.356	-0.070	-0.001	-0.003	-0.098	-0.088	-0.044	c33g12_1
		12	-0.473	-0.201	-0.038	-0.009	-0.030	-0.115	-0.088	-0.050	c33g12_2
	54	6	-0.768	-0.278	-0.046	-0.011	-0.116	-0.129	-0.102	-0.049	c54g6_1
		6	-0.616	-0.261	-0.066	-0.011	-0.121	-0.131	-0.110	-0.050	c54g6_2
		12	-0.307	-0.154	-0.039	-0.008	-0.118	-0.113	-0.098	-0.049	c54g12_1
		12	-0.549	-0.259	-0.037	-0.003	-0.106	-0.123	-0.097	-0.043	c54g12_2
	97	6	-0.283	-0.255	-0.042	-0.003	-0.121	-0.120	-0.098	-0.033	c97g6_1
		6	-0.507	-0.429	-0.061	-0.010	-0.116	-0.122	-0.110	-0.046	c97g6_2
		12	-0.444	-0.143	-0.045	-0.007	-0.075	-0.090	-0.118	-0.049	c97g12_1
		12	-0.714	-0.333	-0.045	-0.007	-0.079	-0.122	-0.105	-0.042	c97g12_2

6. RECOMMENDATIONS

The key envelope response parameters for the lateral (shear) stiffness and strength of stud-fastener-sheathing assemblies are provided in Table 8. These results are based on the cyclic tests. Initial stiffness is determined at $0.40P_{max}$ from the experimental envelope curve. Note, for use in design the variation in the properties should be considered. Typical variation in cold-formed steel strength is on the order of 10% CoV, so variations in excess of this, and as high as 100% or more suggest use of the mean values may not be appropriate in design. An important mitigating factor is that typically many fasteners may be engaged at one time, and thus a large field of fasteners should tend towards mean stiffness and strength. Also note, the limit state for 97 mil studs with OSB sheathing is screw shear, not bearing and pull-through, a different fastener choice (#8 used here) would obviously change this result.

Table 8 Basic response parameter recommendations (per fastener values)

sheathing	steel thickness		initial stiffness	peak load	peak disp
	mil		k_{o-i} kips/in.	P_{max-i} kips	Δ_{max-i} kips
OSB	33	mean	8.5	0.36	0.23
		CoV	18%	12%	8%
	54	mean	12.2	0.44	0.24
		CoV	25%	16%	8%
	97	mean	20.4	0.43	0.09
		CoV	5%	6%	32%
Gypsum	33	mean	3.8	0.10	0.22
		CoV	133%	35%	32%
	54	mean	6.0	0.12	0.56
		CoV	9%	34%	4%
	97	mean	7.1	0.12	0.33
		CoV	143%	178%	13%

For more advanced analysis using the Pinching4 model the parameters provided in Table 9 are recommended. For the backbone curve with OSB sheathing average values (positive and negative) are used from the earlier per-test fitted model (Table 6 and Table 7). This enforces a symmetric response. For the backbone curve with gypsum sheathing, only the negative values are used, thus edge tear out is excluded from the response. (If it is desired to have values for an edge tear out distance of 1.5 in. the positive values may be employed from Table 6 and Table 7). For the unloading/reloading parameters in the Pinching4 model: the OSB sheathed specimens use average values, and the gypsum-

sheathed specimens again use the negative values that preclude edge tear out. For OSB sheathed specimens, cases exist where the optimization routine for the Pinching4 model fitting results in an $rDispN$ parameter that is negative. Negative $rDispN$ are thrown out of the averaging performed for the 33 and 54 mil OSB sheathed specimens and set to zero in the averaging for the 97 mil OSB sheathed specimens. This phenomena is not observed in the model fitting for the gypsum sheathed specimens.

Table 9 Pinching4 model recommendations (per fastener values)

(a) Backbone points

Sheathing		steel thickness 1/1000 in.	Pinching4 Backbone Points																
			$eNd4$ in.	$eNd3$ in.	$eNd2$ in.	$eNd1$ in.	$ePd1$ in.	$ePd2$ in.	$ePd3$ in.	$ePd4$ in.	$eNf4$ kip	$eNf3$ kip	$eNf2$ kip	$eNf1$ kip	$ePf1$ kip	$ePf2$ kip	$ePf3$ kip	$ePf4$ kip	
OSB	33	mean	<i>symmetric</i>					0.020	0.084	0.254	0.493	<i>symmetric</i>				0.16	0.30	0.38	0.026
		CoV						11%	24%	10%	8%					17%	17%	10%	80%
	54	mean						0.020	0.078	0.246	0.414					0.22	0.35	0.46	0.049
		CoV						15%	25%	6%	13%					17%	10%	6%	71%
	97	mean						0.011	0.039	0.082	0.158					0.20	0.39	0.45	0.028
		CoV						9%	15%	23%	32%					8%	10%	13%	81%
Gypsum	33	mean	<i>symmetric</i>					0.010	0.064	0.229	0.601	<i>symmetric</i>				0.04	0.08	0.10	0.022
		CoV						69%	48%	37%	24%					10%	12%	10%	74%
	54	mean						0.008	0.047	0.238	0.560					0.05	0.10	0.12	0.12
		CoV						46%	28%	24%	34%					6%	6%	7%	5%
	97	mean						0.007	0.048	0.290	0.487					0.04	0.11	0.11	0.10
		CoV						43%	18%	42%	37%					17%	8%	14%	25%

(b) unloading and reloading parameters

Sheathing		steel thickness mil	Unloading and reloading Pinching4 Parameters					
			$rDispP$	$rForceP$	$uForceP$	$rDispN$	$rForceN$	$uForceN$
OSB	33	mean	0.41	0.01	0.001	<i>symmetric</i>		
		CoV	21%	-	-			
	54	mean	0.42	0.01	0.001			
		CoV	22%	-	-			
	97	mean	0.29	0.01	0.001			
		CoV	27%	-	-			
Gypsum	33	mean	0.43	0.01	0.001	<i>symmetric</i>		
		CoV	19%	-	-			
	54	mean	0.56	0.01	0.001			
		CoV	4%	-	-			
	97	mean	0.59	0.01	0.001			
		CoV	7%	-	-			

7. CONCLUSIONS

Cold-formed steel stud-fastener-sheathing assemblies were tested in shear under cyclic loads. Steel (stud) thickness, sheathing type, and fastener spacing were varied to determine the effect of these parameters on performance. Steel thickness not only impacts shear strength and stiffness, but also failure mode, ranging from highly ductile response to fastener shear. Sheathing type similarly effects failure mode: pull-through is dominant for OSB and bearing is dominant for gypsum. No significant difference in behaviour is observed between 6 inch and 12 inch fastener spacing. Hysteretic characterization of the stud-fastener-sheathing response using Pinching4 models is provided. The Pinching4 model accurately captures the hysteretic behaviour. Recommended parameters for strength, stiffness, ductility and the complete Pinching4 model parameters across the three stud thicknesses and two sheathing types studied: OSB and gypsum, are provided. The recommended values are encouraged for use in nonlinear models of shear walls built up from basic nonlinear fastener results.

ACKNOWLEDGEMENTS

The authors would like to thank ClarkDietrich for donating the steel studs used in testing. This report was prepared as part of the U.S. National Science Foundation sponsored CFS-NEES project: NSF-CMMI-1041578: NEESR-CR: Enabling Performance-Based Seismic Design of Multi-Story Cold-Formed Steel Structures. The project also received supplementary support and funding from the American Iron and Steel Institute. Project updates are available at www.ce.jhu.edu/cfsnees. Any opinions, findings, and conclusions or recommendations expressed in this publication are those of the author(s) and do not necessarily reflect the views of the National Science Foundation, nor the American Iron and Steel Institute.

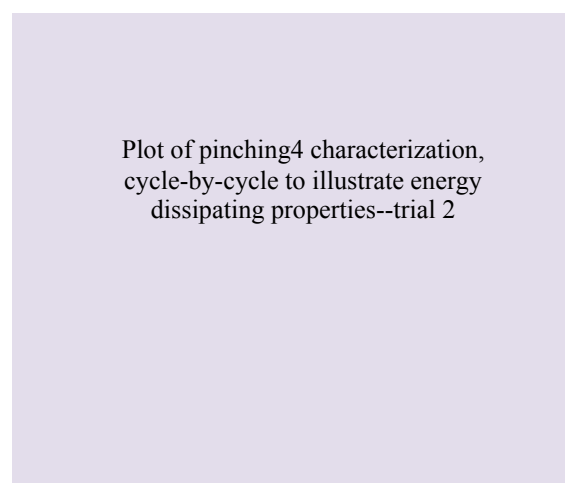
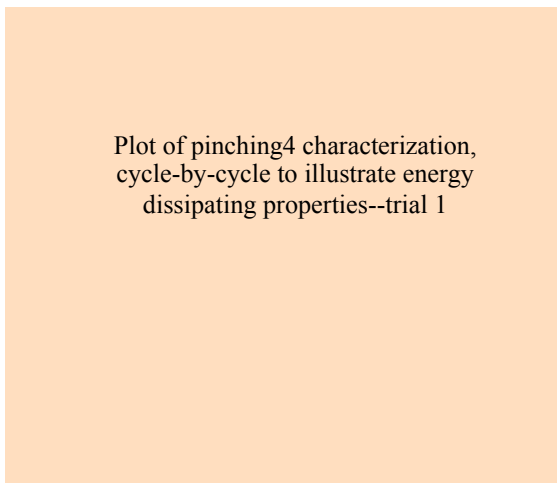
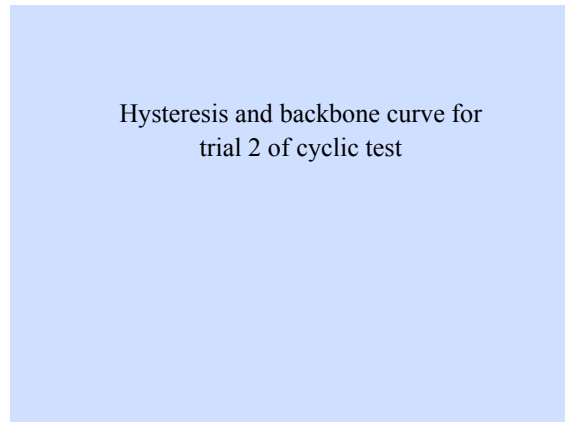
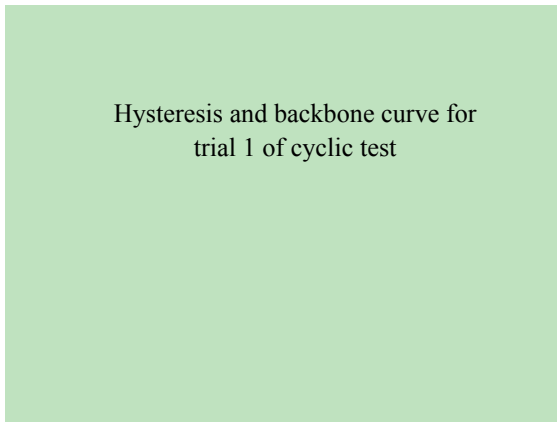
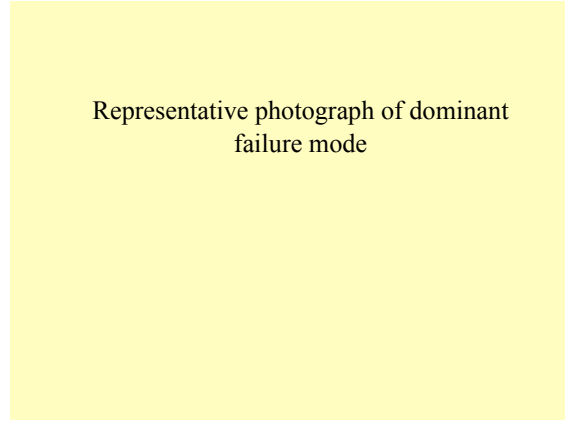
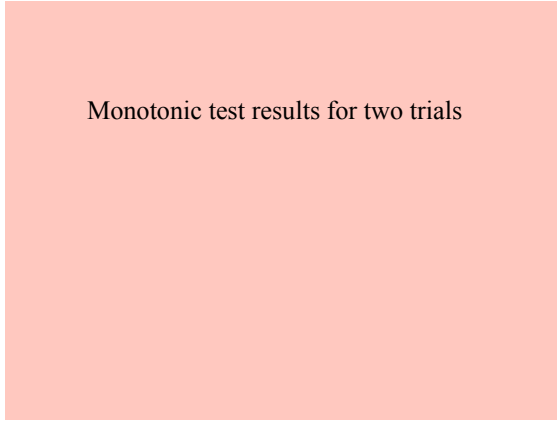
REFERENCES

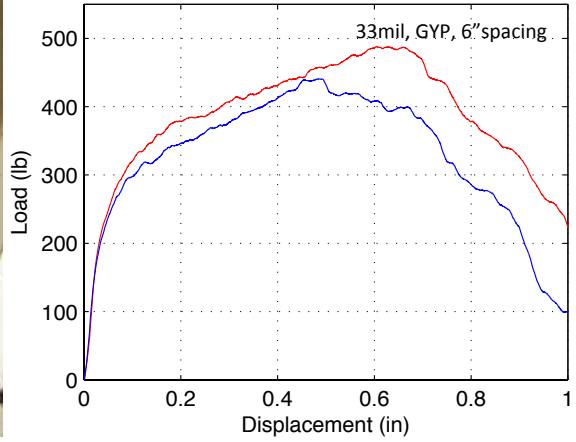
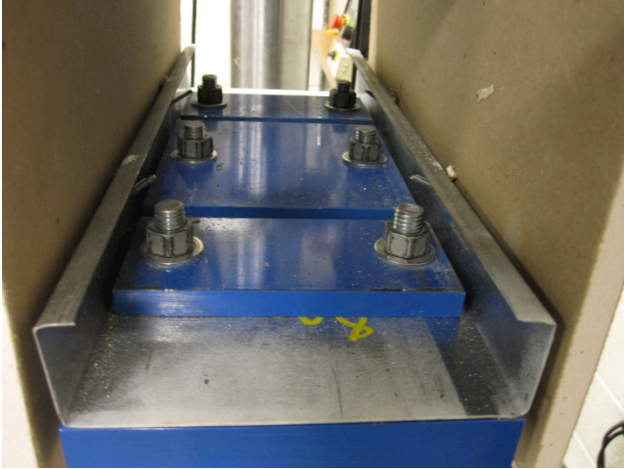
- AISI-S200-07 (2007). North American Standard for Cold-Formed Steel Framing – General Provisions. American Iron and Steel Institute, Washington, D.C., AISI-S200-07.
- AISI-S100-07 (2007). North American Specification for the Design of Cold-Formed Steel Structural Members. American Iron and Steel Institute, Washington, D.C., AISI-S100-07.
- Filiatrault, A., and Folz, B., (2002). Performance-Based Seismic Design of Wood Framed Buildings. *ASCE Journal of Structural Engineering*. **Vol. 128: 1**, 39-47.
- Filiatrault, A., and Folz, B., (2004). Seismic analysis of woodframe structures. I: Model implementation and formulation. *ASCE Journal of Structural Engineering*. **Vol. 130: 9**, 1353-1360.
- Filiatrault, A., and Folz, B., (2004). Seismic analysis of woodframe structures. II: Model implementation and verification. *ASCE Journal of Structural Engineering*. **Vol. 130: 9**, 1361-1370.
- Fiorino, L., Della Corte, G., Landolfo, R. (2007). Experimental tests on typical screw connections for cold-formed steel housing, *Engineering Structures*, **Vol. 29: 8**, 1761-1773.
- Krawinkler H, Parisi F, Ibarra L, Ayoub A, Medina R. (2000). Development of a testing protocol for woodframe structures. Report W-02 covering task 1.3.2, CUREE/Caltech woodframe project.
- Liu, P., Peterman, K.D., Yu, C., Schafer, B.W. (2012). Test report for shear wall tests for the CFS-NEES Building. CFS-NEES-RR01, 2012, www.ce.jhu.edu/cfsnees
- Liu, P., Peterman, K.D., Yu, C., Schafer, B.W. (2012) Cold-formed steel shear walls in ledger-framed buildings. Proceedings of the Annual Stability Conference, Structural Stability Research Council, Dallas, TX, April 2012.
- Lowes, L., Mitra, N., Altoontash, A. (2004). A Beam-Column Joint Model for Simulating the Earthquake Response of Reinforced Concrete Frames. PEER Report 2003/10, www.peer.berkeley.edu.
- Madsen, R.L., Nakata, N., Schafer, B.W. (2011). CFS-NEES Building Structural Design Narrative. CFS-NEES RR01, October 2011, www.ce.jhu.edu/cfsnees.
- Matlab Help Files. "fminsearch." Mathworks, Cambridge MA. 2002.
- Okasha AF. (2004). Performance of steel frame/wood sheathing screw connections subjected to monotonic and cyclic loading. M.Sc. thesis. Montreal: Dept. of Civil Eng. and Applied Mechanics, McGill University.
- Pei, S. and van de Lindt, J. (2010). User's Manual for SAPWood for Windows. www.engr.colostate.edu/NEESWood/SAPwood.htm
- Peterman, K.D., and Schafer, B.W. (2012). CFS-NEES RR04: Test report for fastener stiffness tests for the CFS-NEES Building." CFS-NEES-RR04, 2012, www.ce.jhu.edu/cfsnees
- Vieira, L.C.M., Schafer, B.W. (2009). Experimental Results for Translational Stiffness of Stud-to-Sheathing Assemblies. AISI-COFS Supplemental Report.
- Vieira, L.C.M., Schafer, B.W. (2012). Lateral stiffness and strength of sheathing braced cold-formed steel stud walls, *Engineering Structures*, **Vol. 37**, 205-213.
- Green G.G., Winter G., Cuykendall T.R., Light gage steel columns in wall-braced panels, vol. 35. Cornell University Engineering Experiment Station; 1947. p. 1–50.

APPENDICES

Appendix A: Specimen Information Sheets

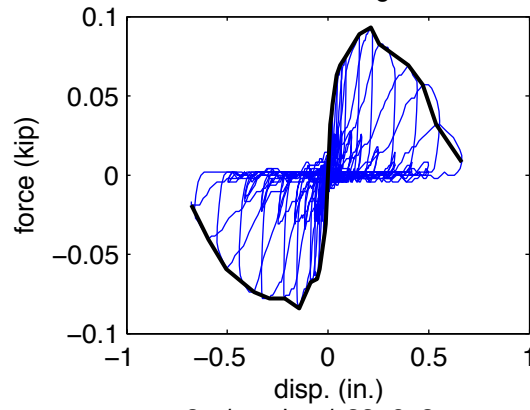
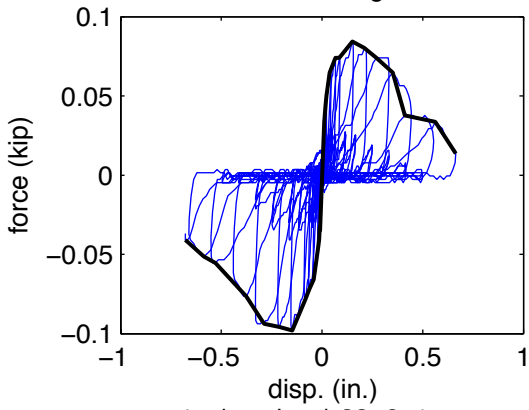
How to read a specimen information sheet:





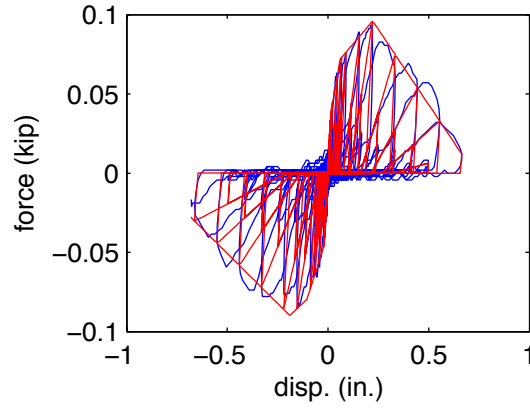
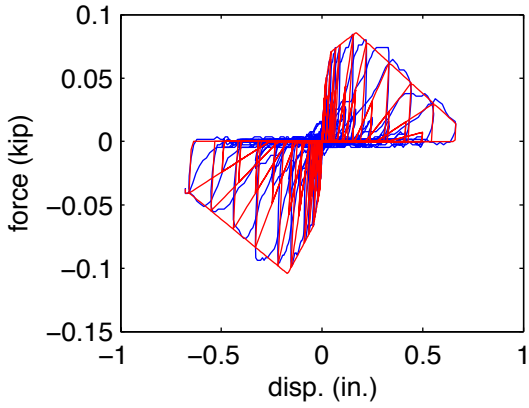
1-./testdata/c33g6_1.txt

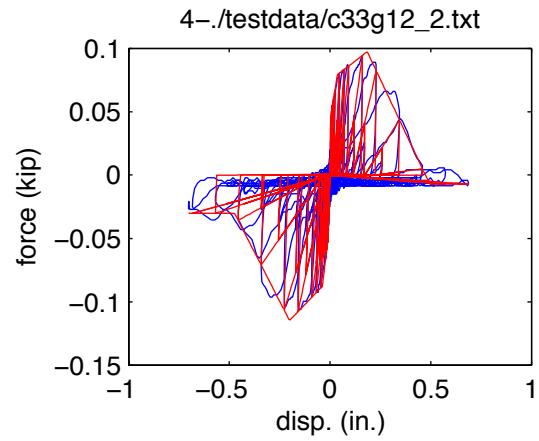
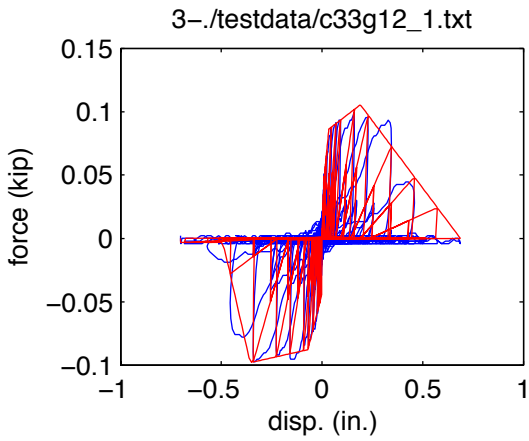
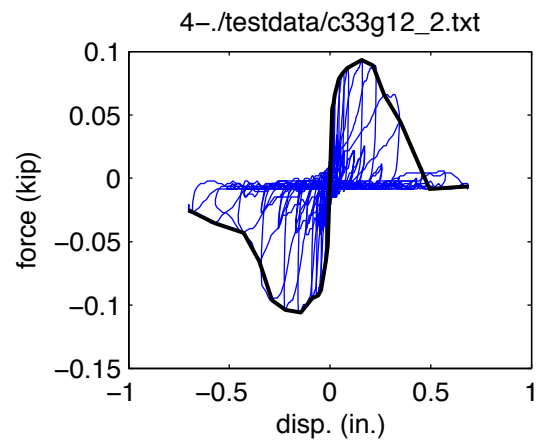
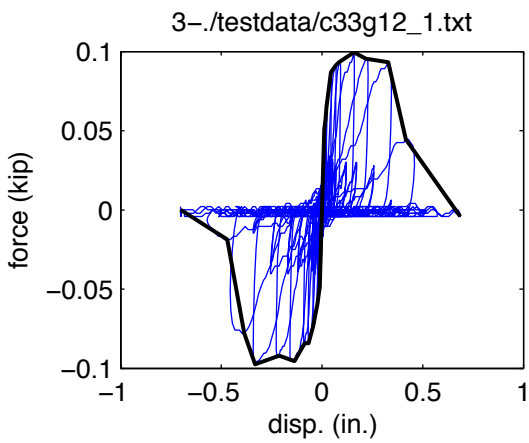
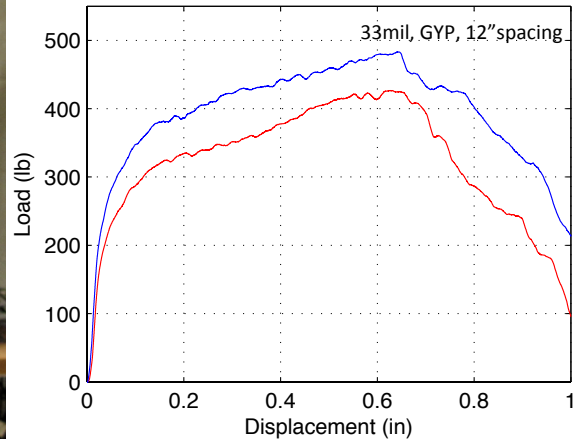
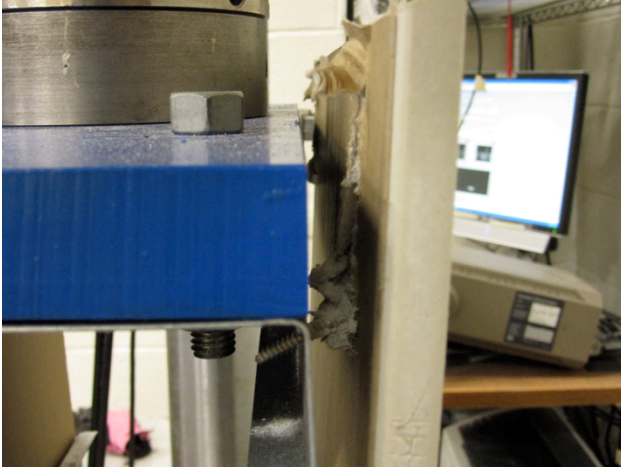
2-./testdata/c33g6_2.txt

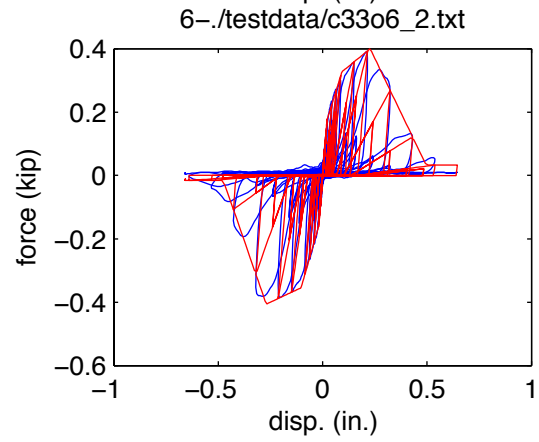
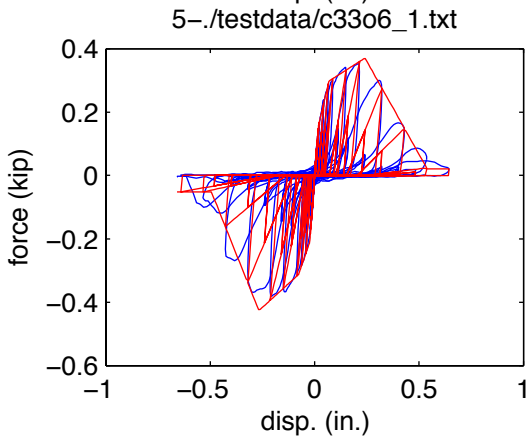
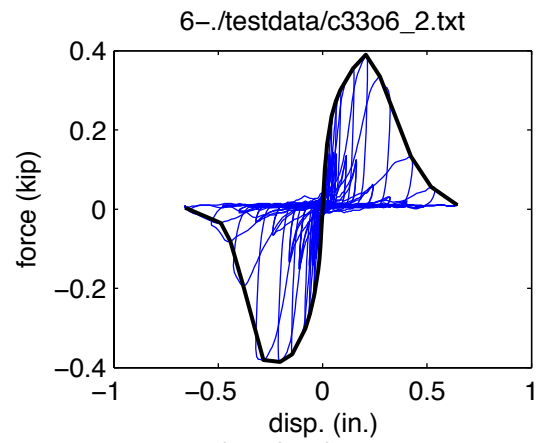
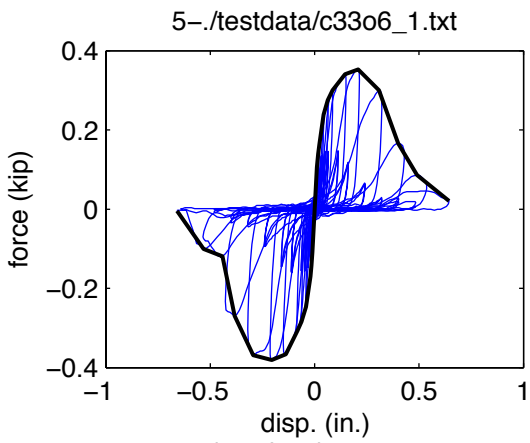
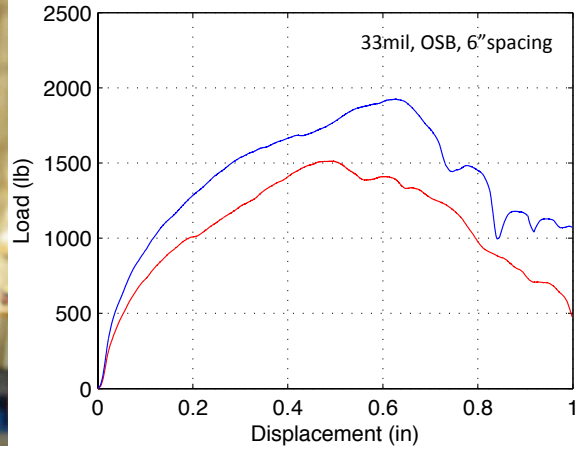


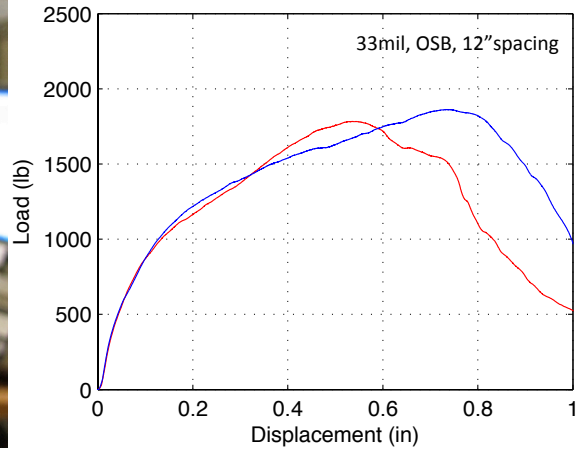
1-./testdata/c33g6_1.txt

2-./testdata/c33g6_2.txt



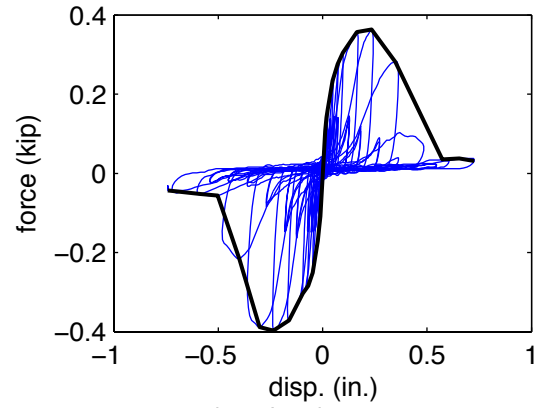
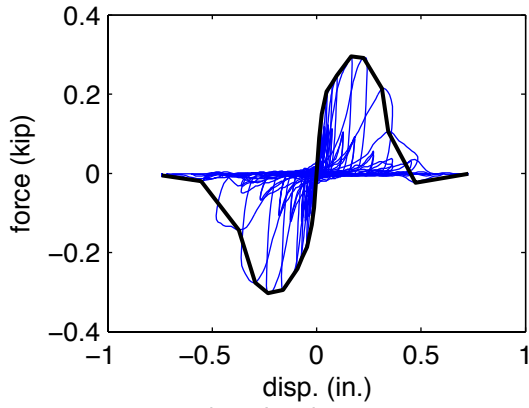






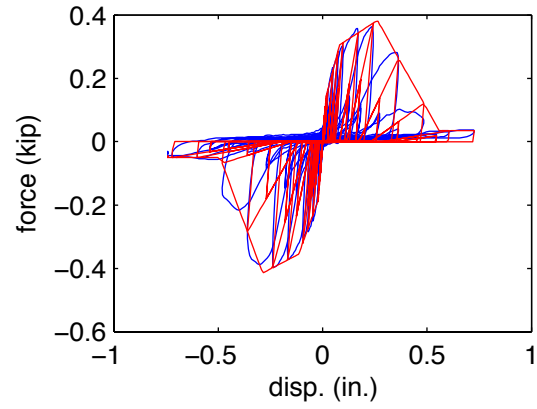
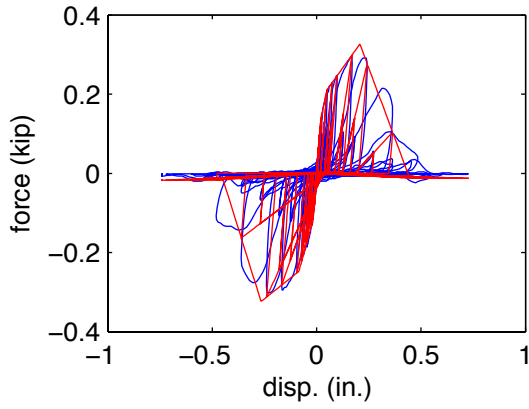
7-./testdata/c33o12_1.txt

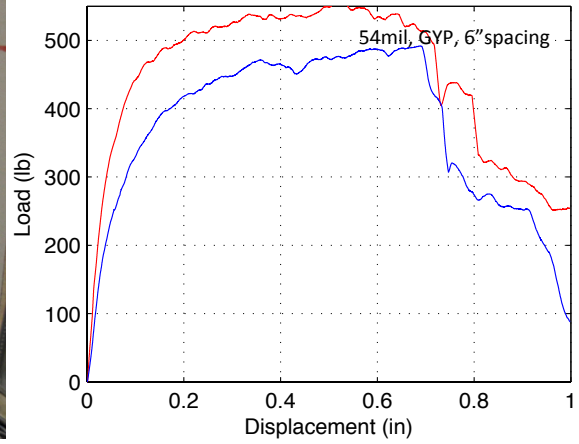
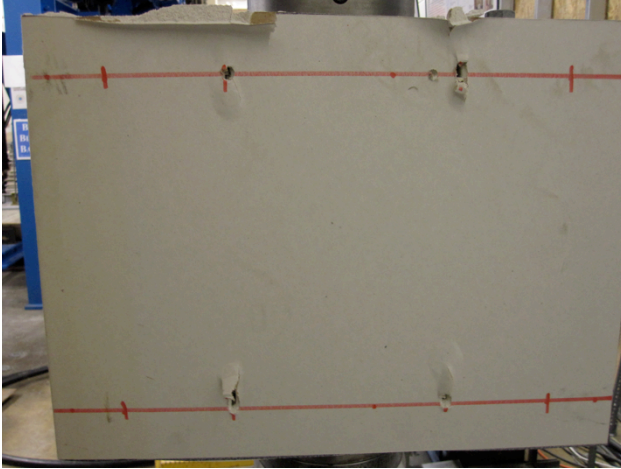
8-./testdata/c33o12_2.txt



7-./testdata/c33o12_1.txt

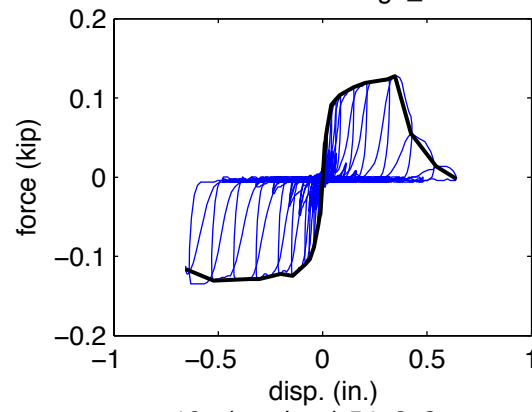
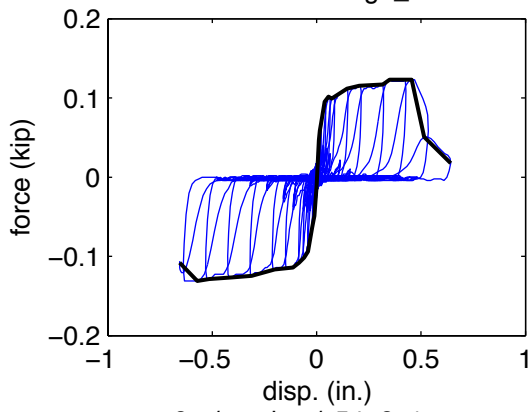
8-./testdata/c33o12_2.txt





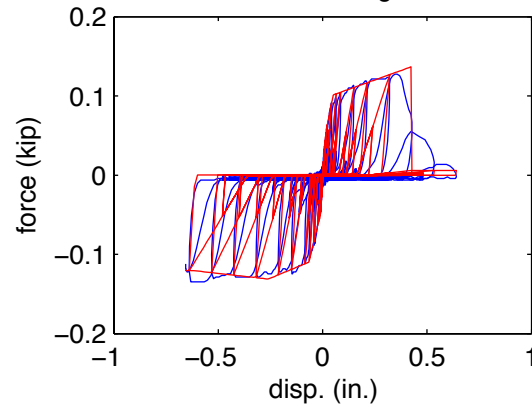
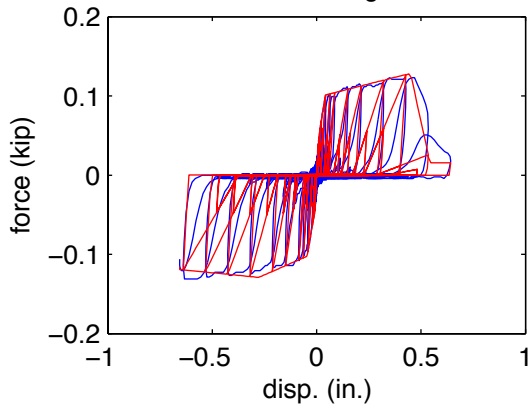
9-./testdata/c54g6_1.txt

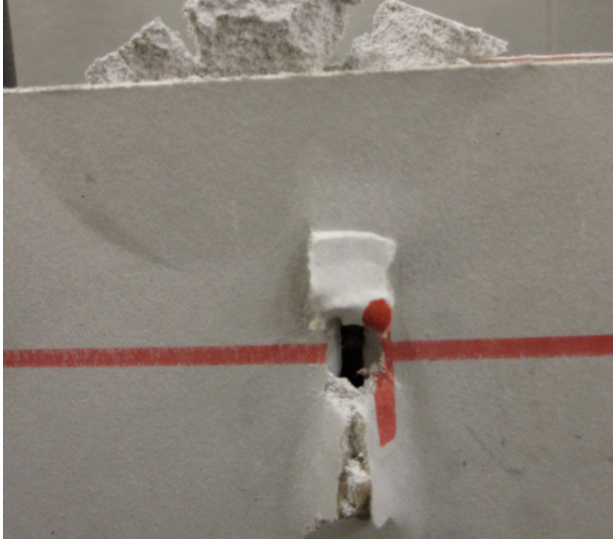
10-./testdata/c54g6_2.txt



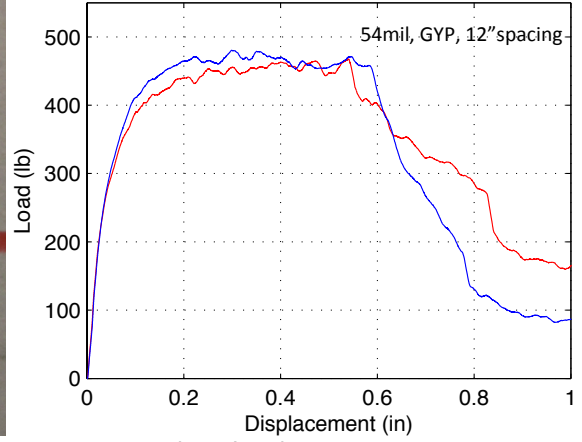
9-./testdata/c54g6_1.txt

10-./testdata/c54g6_2.txt

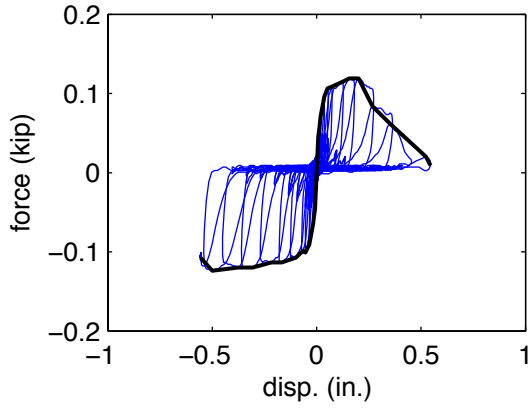




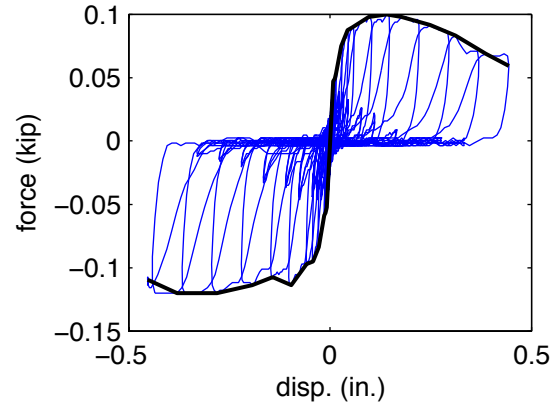
11-./testdata/c54g12_1.txt



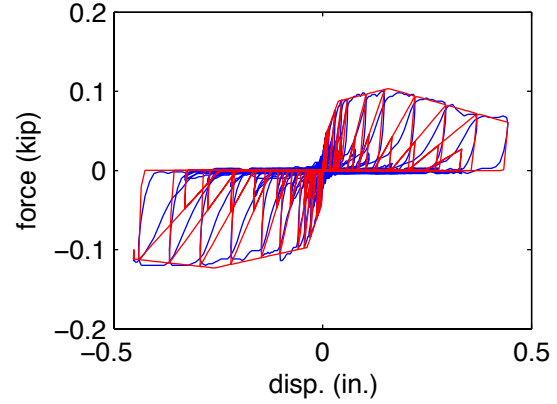
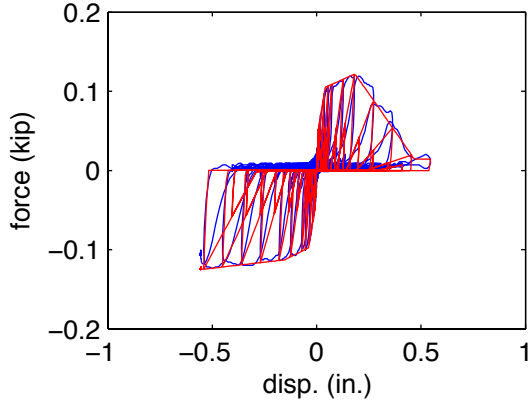
12-./testdata/c54g12_2.txt



11-./testdata/c54g12_1.txt

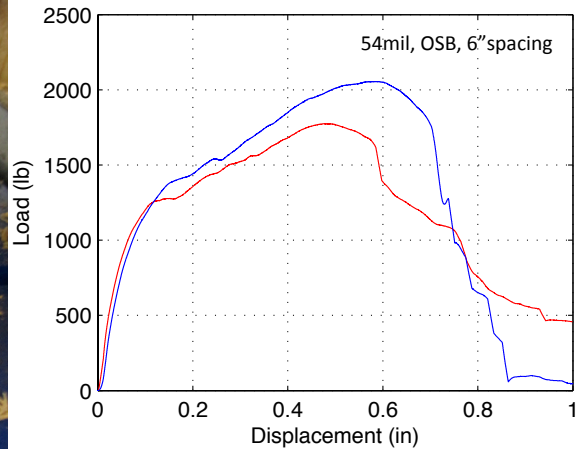


12-./testdata/c54g12_2.txt

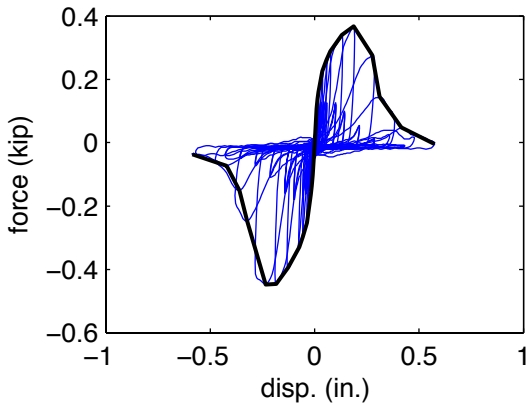




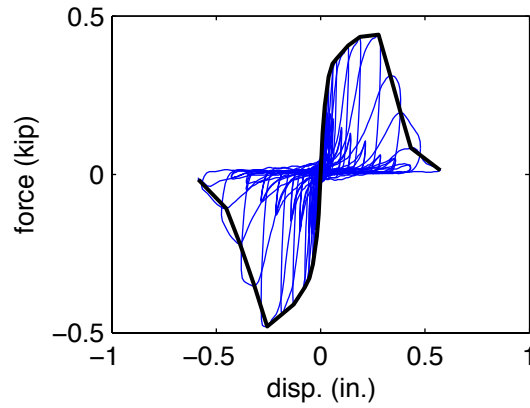
13-./testdata/c54o6_1.txt



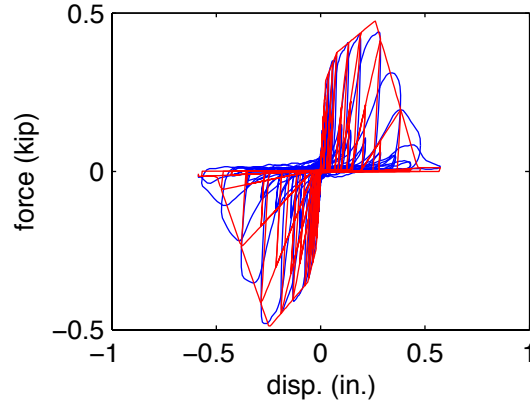
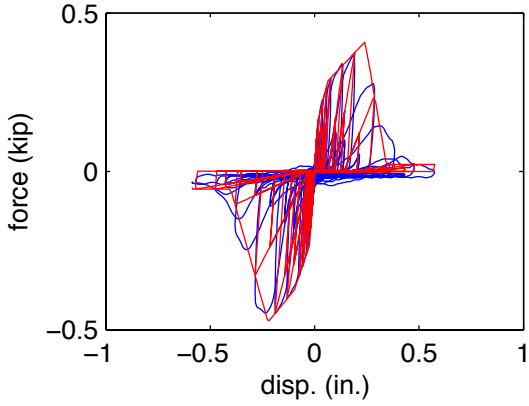
14-./testdata/c54o6_2.txt



13-./testdata/c54o6_1.txt

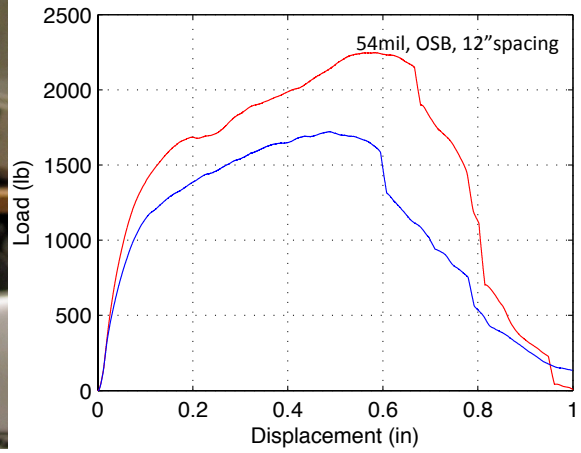


14-./testdata/c54o6_2.txt

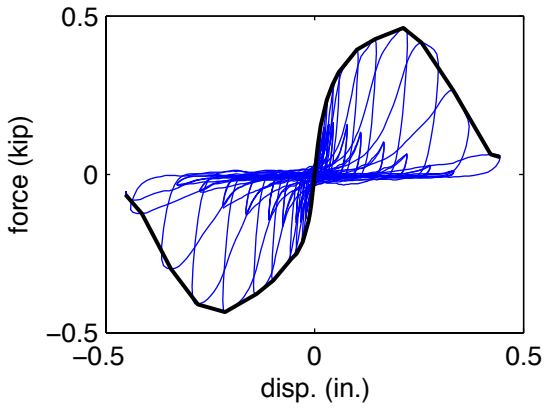




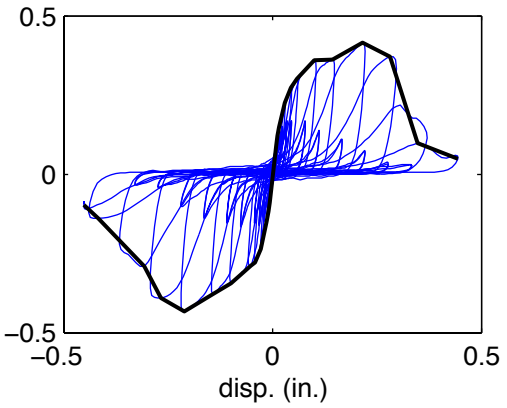
15-./testdata/c54o12_1.txt



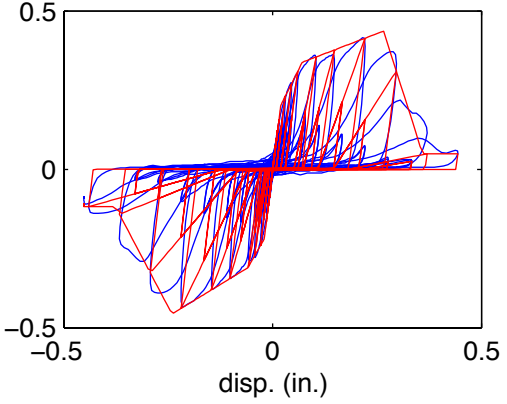
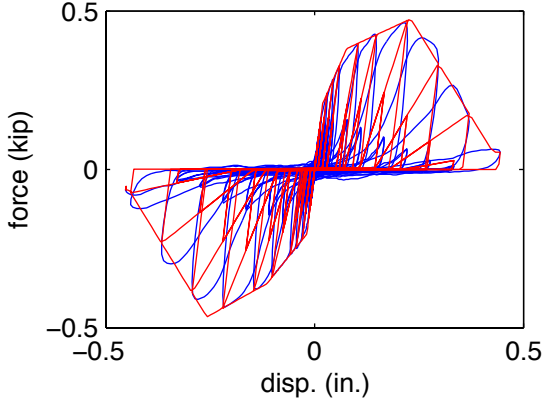
16-./testdata/c54o12_2.txt

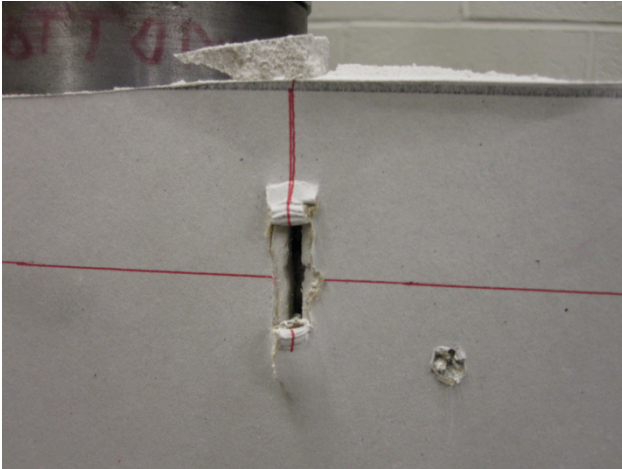


15-./testdata/c54o12_1.txt

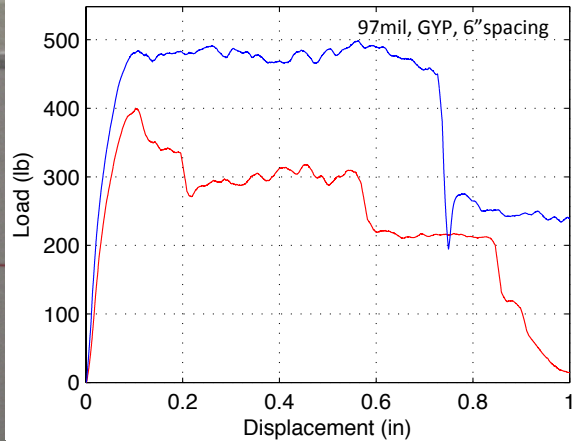


16-./testdata/c54o12_2.txt

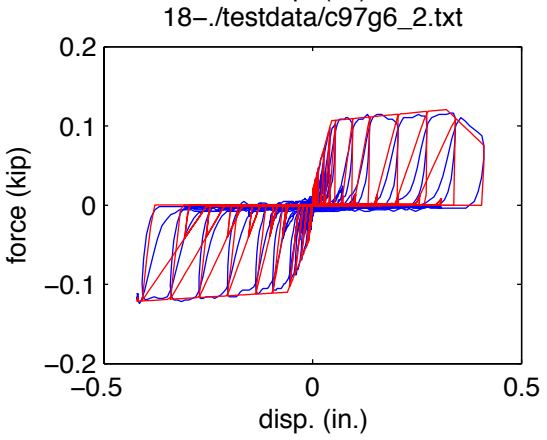
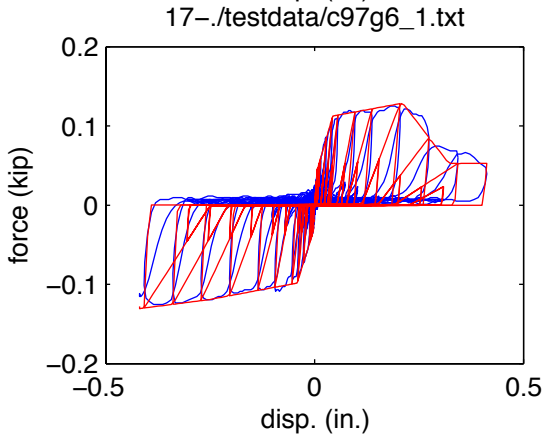
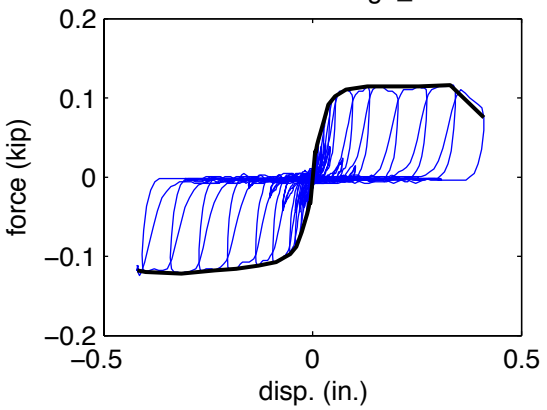
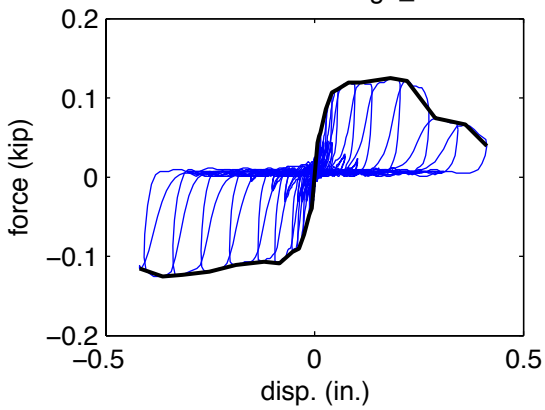


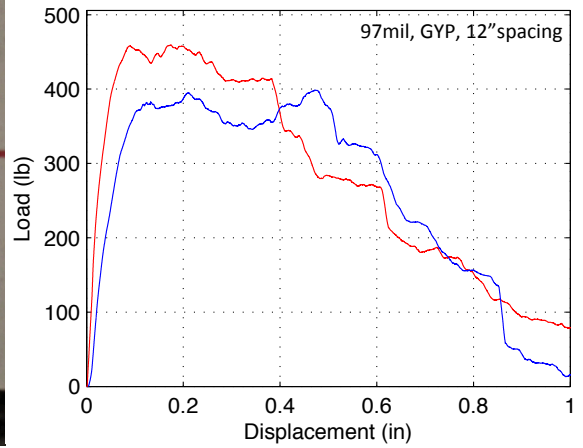
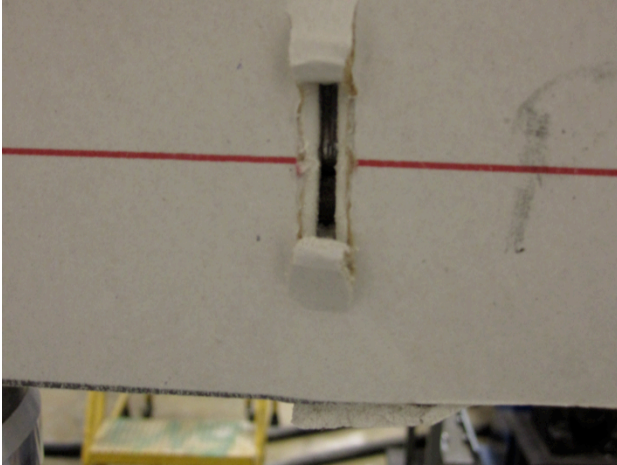


17-./testdata/c97g6_1.txt



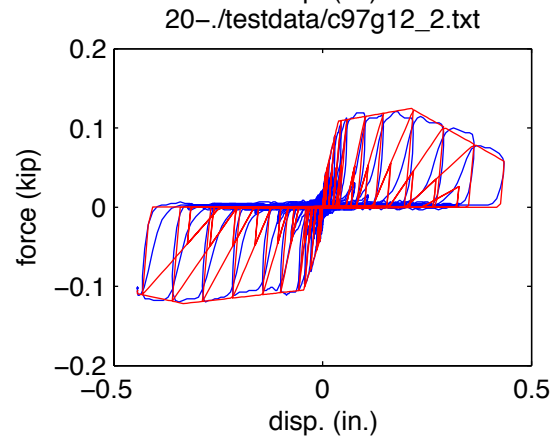
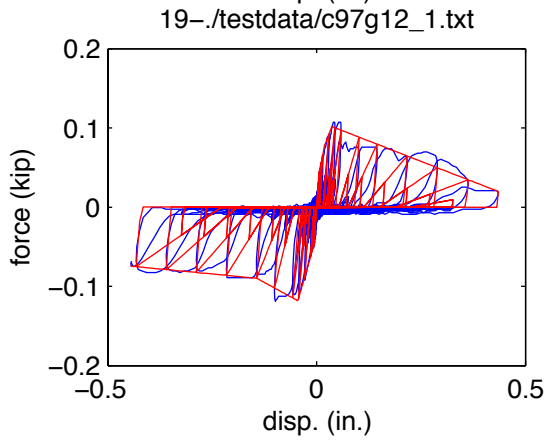
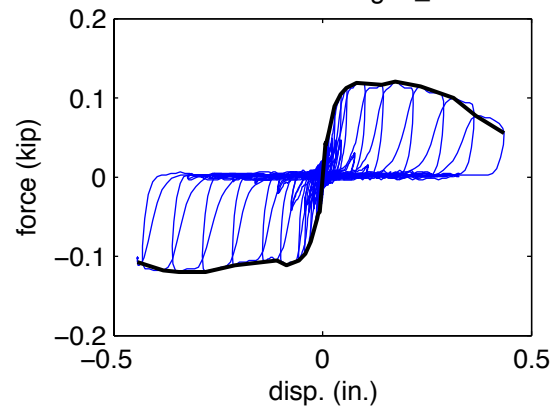
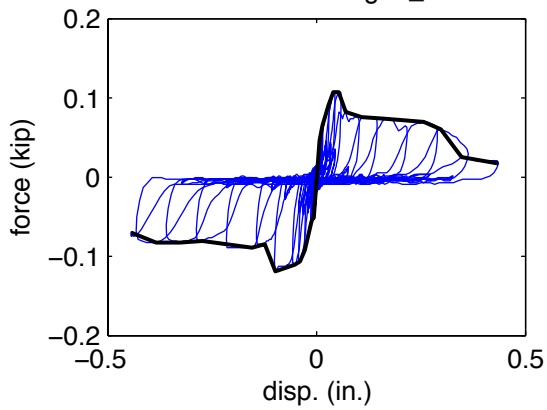
18-./testdata/c97g6_2.txt

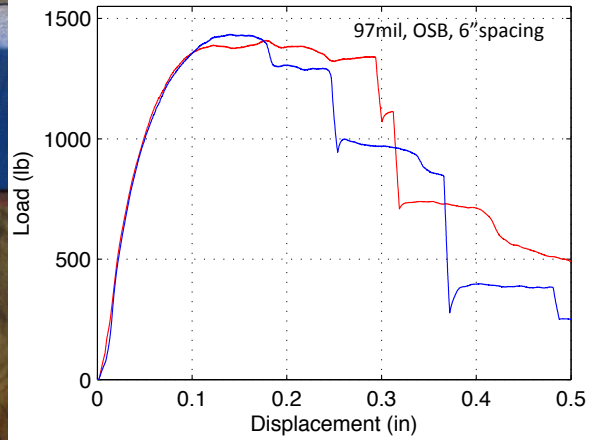




19-./testdata/c97g12_1.txt

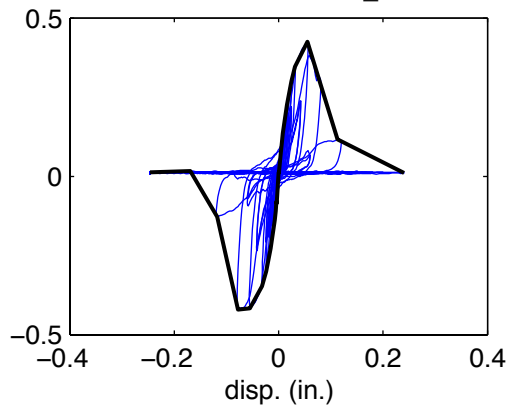
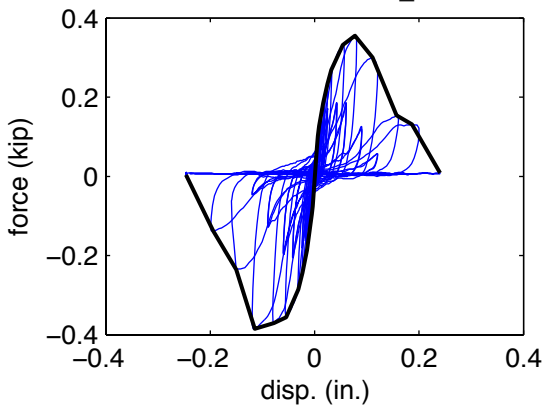
20-./testdata/c97g12_2.txt





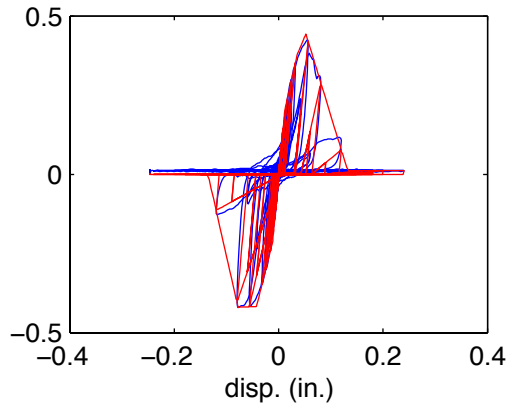
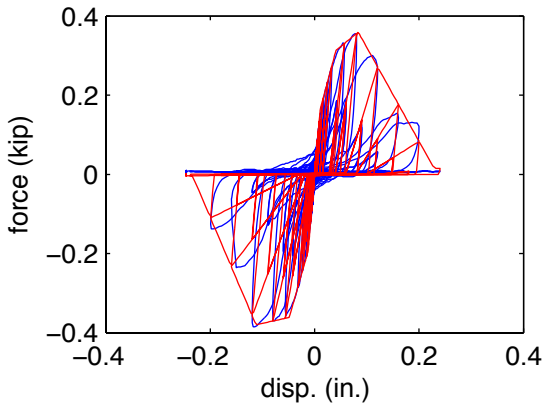
21-./testdata/c97o6_1.txt

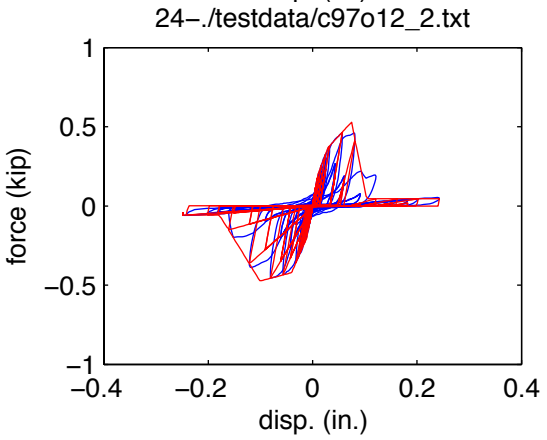
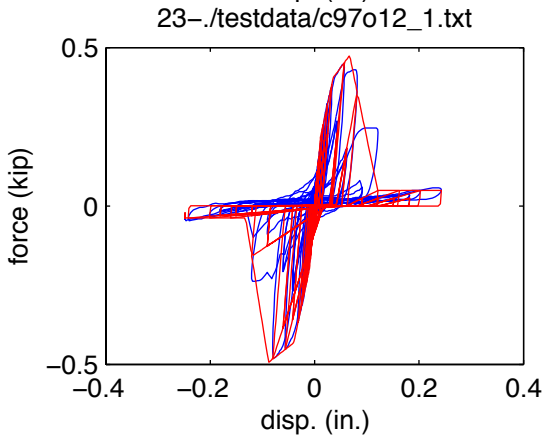
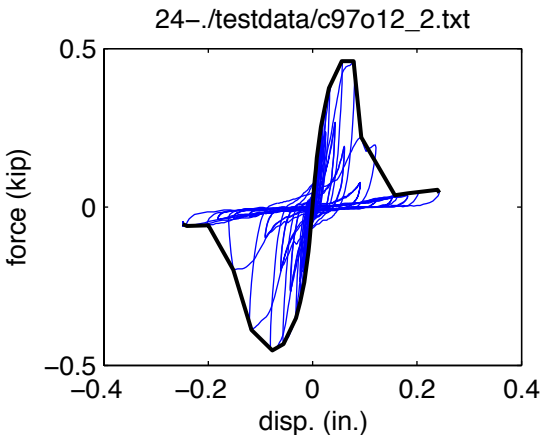
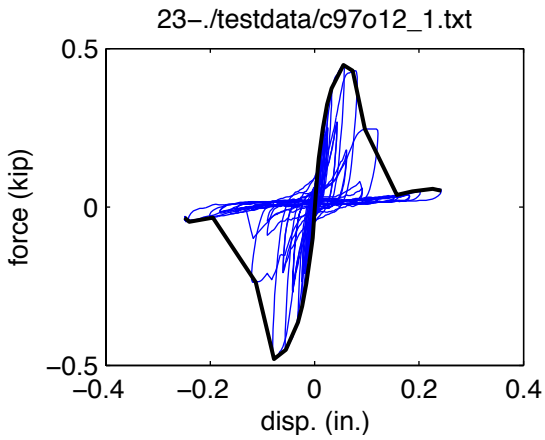
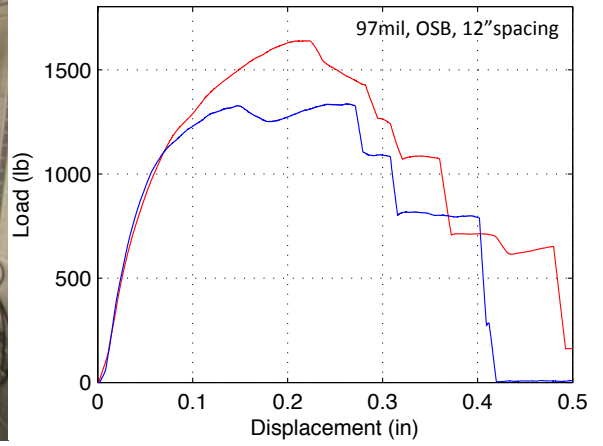
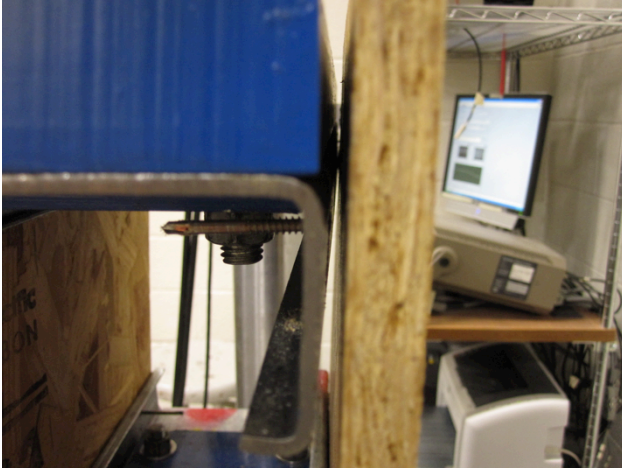
22-./testdata/c97o6_2.txt



21-./testdata/c97o6_1.txt

22-./testdata/c97o6_2.txt





Appendix B: Tensile Test Results

Tensile Test Results

Coupons cut from flanges of channel sections:

-600S162-033 [33ksi]

-600S162-054 [50ksi]

-600S162-097 [50ksi]

